Control Charts based on parameter depths

Ignacio Cascos[a,*], Miguel López-Díaz[b]

[a] *Department of Statistics, Universidad Carlos III de Madrid, UC3M-BS Institute of Financial Big Data, Av. Universidad 30, E-28911 Leganés (Madrid), Spain*
[b] *Departamento de Estadística e I.O. y D.M., Universidad de Oviedo, c/ Federico García Lorca 18, E-33007 Oviedo, Spain*

Abstract

Control charts are designed to monitor on-going production processes by tracking subsequent samples of the production using some statistic of a quality characteristic. We propose to track the *parameter depths* of estimates of a parameter by means of depth (D)-charts, or the associated *depth-based ranks* by means of r-charts. More precisely, given a general parameter (e.g. mean, standard deviation or pair given by mean and standard deviation) and some historical data of the production, the parameter depth of an estimate of the parameter on new samples of the production with regard to the historical data is computed. The process is considered to be out-of-control when the depth of the estimate of the parameter falls below some given threshold (control limit). Some control limits of specific D-charts are obtained under the assumption of normality of the quality characteristic.

Keywords: Depth-based rank, Parameter depth, Statistical process control, Zonoid depth, (μ, σ)-depth

1. Introduction

Given a probability distribution or a data cloud, a data depth function assesses the degree of centrality of each point of the corresponding Euclidean space with respect to it, see [1, 2, 3, 4, 5]. The notion of *parameter depth* is an extension of the one of data depth. Specifically, for any element of a parameter space, its parameter depth with respect to a probability distribution, assesses how well does it fit the given distribution as a parameter, see [6, 7]. Consider for example a point $(m, s) \in \mathbb{R} \times [0, +\infty)$ which is a candidate to be a location-scale parameter of a univariate dataset. The better (m, s) fits the dataset as a location-scale parameter, the greater its *location-scale (parameter) depth* would be. The notion of parameter depth is broader than the one of data depth since any data depth is clearly a parameter depth for a location parameter.

The second main ingredient in this manuscript are control charts, which are used to monitor on-going production processes, see e.g. Montgomery [8]. The quality of the production is identified

*Ph. (+34) 91 624 8750, Fax: (+34) 91 624 9177
Email addresses: ignacio.cascos@uc3m.es (Ignacio Cascos), mld@uniovi.es (Miguel López-Díaz)

with a quantitative characteristic, and the evolution of such a characteristic over subsequent samples is tracked. The aim of a control chart is to detect the presence of abnormalities (assignable causes) in the production process by raising an alarm whenever the quality characteristic of the production departs from a prescribed distribution. In such a case, the process is said to be *out-of-control*, while otherwise it is in the *in-control* state.

The most common control chart is Shewart $\overline{X}$-chart that tracks the evolution of the sample mean of a univariate process over rational samples of size k. The control limits are set at $\mu_0 \pm t\sigma_0/\sqrt{k}$, where μ_0 and σ_0 are the in-control mean and standard deviation. It is commonly assumed that the quality characteristic is normally distributed and t is set at the $(1-\alpha/2)$-quantile of a standard normal distribution, $z_{\alpha/2}$, which results in raising an alarm (sample mean not within control limits) despite the process has not departed from the prescribed distribution with probability α (false alarm rate). The canonical value of $t = z_{\alpha/2}$ is 3 and it results in $\alpha = 0.0027$. When the quality characteristic is non-normal, some alternative charts to monitor the sample mean have been proposed, either for a quality characteristic from a given family of distributions, see [9], or for distributions with a given shape, see [10] for skewed ones, to mention just two.

Charts for averages are commonly used in combination with other charts that monitor the variability of the quality characteristic, either by means of sample ranges or sample standard deviations. The canonical charts here are the R and S-charts that can be found, e.g., in [8]. Nevertheless there exist charts built to monitor the scale when the quality characteristic is skewed, see [11], or when it follows some prescribed distribution, see [12].

For a multivariate quality characteristic, the generalization of the $\overline{X}$-chart appears in the for of the Hotelling T^2-chart, see [8], which is built under assumption of normality, but there exist some modifications of this chart specifical for skewed populations, see [13].

Liu [14] designed nonparametric control charts for multivariate distributions based on the ranks of individual observations that are induced by a notion of data depth. Her work was later extended to parametric models by Liu and Singh [15] who propose to build artificial samples on a given parameter space and has been recently revisited by Bell *et al.* [16]. Akin to the previous approaches, Ciupke [17] has proposed a multivariate capability index based on a modified tolerance region which is obtained after dilating the set of all points whose data depth is at least some given value (depth-trimmed region).

Specifically, our proposal consists in monitoring an on-going process by tracking the parameter depths of estimates of a parameter obtained over subsequent rational samples of the production. The process is considered to be out-of-control when the depth of the estimate of the parameter falls below some given threshold and the in-control region is thus a depth-trimmed region.

In the current manuscript special attention will be devoted to control charts for joint monitorization of location and scale. Other proposals in this direction can be found in Chao and Cheng [18] and McCracken and Chakraborti [19], who consider the joint monitorization of mean and variance, and in Mukherjee and Chakraborti [20] and Chowdhury *et al.* [21], who consider nonparametric alternatives based on univariate ranks. Adaptive control schemes with memory for

joint monitorization of location and scale have been also proposed, see Yang [22].

In Section 2 some notions of parameter depth are introduced, together with the ranks based on them. Section 3 is devoted to nonparametric control charts for depths and ranks. In Section 4 the exact control limits of the D-charts that track the sample mean, the sample standard deviation, and the pair given by sample mean and sample standard deviation are computed under the assumption of normality, while several applications and examples are presented in Section 5. Section 6 is devoted to compare our charts with other existing ones either by means of their Operating Characteristic curves or their respective Average Run Lengths when the quality distribution has suffered some given shit on its parameters. Section 7 contains two real-data applications, one for a univariate non-normal process, and the other for a multivariate normal process. Some concluding remarks are finally presented in Section 8 and an Appendix containing tables with control limits of D-charts for normal processes is included after the bibliographic references.

2. Preliminaries: parameter depths and ranks

We start defining the parameter depth functions that will be used throughout the manuscript and then introduce the ranks induced by them.

2.1. Parameter depth-trimmed regions

Let $\mathbb{P}$ denote the set of probability measures on the p-dimensional Euclidean space $\mathbb{R}^p$ equipped with the Borel σ-algebra. For any functional of a probability distribution (parameter) $\theta : \mathbb{P} \mapsto \mathbb{R}^q$, Cascos and López-Díaz [6] define the *parameter depth-trimmed region* of level $d \in (0, 1]$ induced by θ as

$$\mathrm{D}^d_\theta(P) = \{\theta(Q) : Q \in \mathbb{P} \text{ with } Q(A) \leq d^{-1}P(A)\,, \text{ for all Borelian } A \subset \mathbb{R}^p\}\,. \tag{1}$$

For any dimension p, if θ represents the mean, $\mu(P) = \int x \mathrm{d}P$, equation (1) leads to the *zonoid trimmed regions* thoroughly studied by Koshevoy and Mosler [23]. Hereafter, we will refer to such trimmed regions as μ-trimmed regions. If $p = 1$ and the chosen functional is the standard deviation, $\sigma(P) = \left(\int x^2 \mathrm{d}P - \mu(P)^2\right)^{1/2}$, we obtain the σ-trimmed regions, and for the two-dimensional parameter (μ, σ), we obtain the (μ, σ)-trimmed regions.

Alternative equivalent expressions for the μ-, σ-, and (μ, σ)-trimmed regions are given below

$$\begin{aligned}
\mathrm{D}^d_\mu(P) &= \left\{ \int \boldsymbol{y} g(\boldsymbol{y}) \mathrm{d}P(\boldsymbol{y}), \text{ for some } g : \mathbb{R}^p \mapsto [0, d^{-1}] \text{ measurable}, \int g(\boldsymbol{y}) \mathrm{d}P(\boldsymbol{y}) = 1 \right\};\\
\mathrm{D}^d_\sigma(P_X) &= \{s : \ (m, m^2 + s^2) \in \mathrm{D}^d_\mu(P_{(X,X^2)}) \text{ for some } m \in \mathbb{R}\};\\
\mathrm{D}^d_{\mu,\sigma}(P_X) &= \{(m, s) : (m, m^2 + s^2) \in \mathrm{D}^d_\mu(P_{(X,X^2)})\},
\end{aligned}$$

where P_X and $P_{(X,X^2)}$ are respectively the probability distributions induced by the random variable X and the bivariate random vector (X, X^2).

The μ-trimmed region of level d of a continuous random variable X can be written as

$$\mathrm{D}^d_\mu(P_X) = \left[\frac{1}{d} \int_{-\infty}^{F_X^{-1}(d)} x f_X(x) \mathrm{d}x\,,\ \frac{1}{d} \int_{F_X^{-1}(1-d)}^{+\infty} x f_X(x) \mathrm{d}x \right], \tag{2}$$

where F_X^{-1} stands for the quantile function of X and f_X for its density mass function.

Equivariance properties. For any $q \times p$ nonsingular matrix $\boldsymbol{A}$, point $\boldsymbol{b} \in \mathbb{R}^q$, and scalars $a, b \in \mathbb{R}$, the following equivariance properties hold true

1. $\mathrm{D}_\mu^d(P_{\boldsymbol{A}X+\boldsymbol{b}}) = \{\boldsymbol{A}\boldsymbol{x} + \boldsymbol{b} : \boldsymbol{x} \in \mathrm{D}_\mu^d(P_X)\}$ for any p-dimensional random vector X;
2. $\mathrm{D}_\sigma^d(P_{aX+b}) = \{|a|x : x \in \mathrm{D}_\sigma^d(P_X)\}$ for any random variable X;
3. $\mathrm{D}_{\mu,\sigma}^d(P_{aX+b}) = \{(ax + b, |a|y) : (x, y) \in \mathrm{D}_{\mu,\sigma}^d(P_X)\}$ for any random variable X.

The empirical trimmed regions are obtained after substituting probability P by the empirical probability $\hat{P}_n$ built out of a sample of X of size n. Observe that for $d = 1$, we obtain

$$\mathrm{D}_\mu^1(\hat{P}_n) = \{\overline{X}\} \qquad , \qquad \mathrm{D}_\sigma^1(\hat{P}_n) = \{S_n\} \qquad , \qquad \mathrm{D}_{\mu,\sigma}^1(\hat{P}_n) = \{(\overline{X}, S_n)\}\,,$$

where S_n is the square root of the not bias-corrected sample variance, which we will denote by S_n^2. In general $\mathrm{D}_\theta^1(\hat{P}_n) = \{\hat{\theta}_n\}$, where $\hat{\theta}_n = \theta(\hat{P}_n)$ is the plug-in estimator of θ based on the empirical distribution.

Consistency. Since the distribution of the quality characteristic is to be estimated from historical data and depth-trimmed regions will serve as in-control regions, their consistency is a crucial issue. As long as the first moment (resp. second moment) of P is finite, the empirical depth-trimmed regions associated with μ (resp. σ) are consistent estimators of the corresponding population ones, see Cascos and López-Díaz [6, 24]. When θ is either of μ, σ or (μ, σ) it holds *a.s.* that

$$\lim \mathrm{D}_\theta^d(\hat{P}_n) = \mathrm{D}_\theta^d(P)\,. \tag{3}$$

2.2. Parameter depths

The depth function induced by any of the previous families of depth-trimmed regions evaluated at $\boldsymbol{\theta}_0$ (an element of the parameter space) is given by $\mathrm{D}_\theta(\boldsymbol{\theta}_0; P) = \sup\{d \in (0, 1] : \boldsymbol{\theta}_0 \in \mathrm{D}_\theta^d(P)\}$. Observe that the depth of $\boldsymbol{\theta}_0$ is one minus the smallest fraction of probability mass that must be blurred from P in order to obtain (after appropriate rescaling) a new probability distribution Q whose parameter θ assumes value $\boldsymbol{\theta}_0 = \theta(Q)$.

For the particular instances that are relevant to us, we have:

$$\mathrm{D}_\mu(\boldsymbol{x}; P) = \sup\left\{d \in (0, 1] : \boldsymbol{x} = \int \boldsymbol{y} g(\boldsymbol{y}) \mathrm{d}P(\boldsymbol{y}), \qquad g : \mathbb{R}^p \mapsto [0, d^{-1}] \text{ measurable}, \right.$$
$$\left. \int g(\boldsymbol{y}) \mathrm{d}P(\boldsymbol{y}) = 1\right\}; \tag{4}$$

$$\mathrm{D}_\sigma(s; P_X) = \sup_m \mathrm{D}_\mu\big((m, m^2 + s^2); P_{(X,X^2)}\big)\,; \tag{5}$$

$$\mathrm{D}_{\mu,\sigma}\big((m, s); P_X\big) = \mathrm{D}_\mu\big((m, m^2 + s^2); P_{(X,X^2)}\big)\,. \tag{6}$$

The sample (zonoid) μ-depth (4) in dimension $p = 1$ is simple to compute, it amounts to the largest fraction of observations such that x is its average value. Clearly such observations should be consecutive in the ordered sample and either include the smallest (if x is less than the total average) or the largest. The multivariate sample μ-depth can be computed with the R package `ddalpha`, see Pokotylo *et al.* [25]. As seen in (6), the (μ, σ)-depth is a special case of the bivariate μ-depth and thus can be also computed with `ddalpha`. Finally, the σ-depth (5) is the solution to a maximization problem associated with the (μ, σ)-depth.

Invariance properties. For any $p \times p$ nonsingular matrix $\boldsymbol{A}$, points $\boldsymbol{x}, \boldsymbol{b} \in \mathbb{R}^p$, scalars $0 \neq a, x, b \in \mathbb{R}$, and $s > 0$, the following invariance properties hold true

1. $\mathrm{D}_\mu(\boldsymbol{A}\boldsymbol{x} + \boldsymbol{b}; P_{\boldsymbol{A}X+\boldsymbol{b}}) = \mathrm{D}_\mu(\boldsymbol{x}; P_X)$ for any p-dimensional random vector X;
2. $\mathrm{D}_\sigma(|a|s; P_{aX}) = \mathrm{D}_\sigma(s; P_X)$ for any random variable X;
3. $\mathrm{D}_{\mu,\sigma}((ax + b, |a|s); P_{aX+b}) = \mathrm{D}_{\mu,\sigma}((x, s); P_X)$ for any random variable X .

Another relevant property of the μ-depth is that the depth of $\boldsymbol{x} \in \mathbb{R}^p$ with respect to a p-dimensional random vector X can be obtained in terms of univariate μ-depths as the *projection infimum*, see [26, Th. 4.7]

$$\mathrm{D}_\mu(\boldsymbol{x}; P_X) = \inf_{\boldsymbol{u} \in \mathbb{R}^p} \mathrm{D}_\mu(\langle \boldsymbol{x}, \boldsymbol{u} \rangle; P_{\langle X, \boldsymbol{u} \rangle}) \,. \tag{7}$$

Continuity and (uniform) consistency. The usage of depth-based ranks is justified by the continuity of the depth functions, while the one of the empirical rank, by its uniform consistency.

- *Continuity:* $\mathrm{D}_\theta(\boldsymbol{y}_n; P) \longrightarrow_n \mathrm{D}_\theta(\boldsymbol{y}; P)$ if $\boldsymbol{y}_n \to_n \boldsymbol{y}$,

  holds for the μ-depth on points with strictly positive depth, see Koshevoy and Mosler [23, Th. 7.1(ii)], consequently also for the σ-depth and for the (μ, σ)-depth under the same conditions.

- *Uniform consistency:* $\sup_{\boldsymbol{y}} |\mathrm{D}_\theta(\boldsymbol{y}; \hat{P}_n) - \mathrm{D}_\theta(\boldsymbol{y}; P)| \longrightarrow_n 0$ a.s.,

  holds for the μ-depth as long as P assesses probability zero to the boundaries of all halfspaces with probability one, see Cascos and López-Díaz [27], and consequently for the (μ, σ)-depth as long as P is absolutely continuous.

2.3. Depth-based ranks

Ranking multivariate observations. Liu and Singh [28] defined the depth-based rank of a p-dimensional observation $\boldsymbol{x} \in \mathbb{R}^p$ with respect to a probability distribution P on $\mathbb{R}^p$ as

$$r_P(\boldsymbol{x}) = \Pr\{Y : \mathrm{D}(Y; P) \leq \mathrm{D}(\boldsymbol{x}; P)\} \,, \tag{8}$$

where Y is distributed as P, and D is any data depth function, e.g. the μ-depth.

This depth-based rank was used by Liu [14] to build the so-called r and Q charts which respectively monitor the evolution of the depth-based rank of individual observations and average depth-based rank of the observations of a sample (multivariate generalization of the $\overline{X}$-chart).

Ranking elements of parameter space. We define the *parameter rank* of an element $\boldsymbol{\theta}_0$ of a parameter space with respect to a parameter θ, a sample of size k, and a probability distribution P as

$$r_P^{\theta,k}(\boldsymbol{\theta}_0) = \Pr\{(Y_1,\ldots,Y_k) : \mathrm{D}_\theta(\hat{\theta}(Y_1,\ldots,Y_k);P) \leq \mathrm{D}_\theta(\boldsymbol{\theta}_0;P)\}\,, \tag{9}$$

where $Y_1,\ldots,Y_k$ is a random sample of P of size k and, unless it is explicitly defined somehow else, $\hat{\theta}$ is the plug-in estimator of θ based on the empirical distribution function, i.e. $\hat{\theta}(Y_1,\ldots,Y_k) = \theta(\hat{P}_k)$, where $\hat{P}_k$ is the empirical probability associated with the sample $Y_1,\ldots,Y_k$.

In order to estimate the *parameter rank* of $\boldsymbol{\theta}_0$ from a sample of size n, $X_1,\ldots,X_n$, we consider the rank of $\boldsymbol{\theta}_0$ with respect to the empirical probability $\hat{P}_n$,

$$r_{\hat{P}_n}^{\theta,k}(\boldsymbol{\theta}_0) = \frac{\#\{1 \leq i_1,\ldots,i_k \leq n : \mathrm{D}_\theta(\hat{\theta}(X_{i_1},\ldots,X_{i_k});\hat{P}_n) \leq \mathrm{D}_\theta(\boldsymbol{\theta}_0;\hat{P}_n)\}}{n^k}\,. \tag{10}$$

For large values of n, even for not so large values of k, the computation of $r_{\hat{P}_n}^{\theta,k}(\boldsymbol{\theta}_0)$ becomes computationally unaffordable, and we must estimate $r_{\hat{P}_n}^{\theta,k}(\boldsymbol{\theta}_0)$ resampling from $X_1,\ldots,X_n$. Consider N bootstrap samples $X_{1,i}^*,\ldots,X_{k,i}^*$ of size k drawn with replacement from $X_1,\ldots,X_n$, and let $\theta_i^* = \hat{\theta}(X_{1,i}^*,\ldots,X_{k,i}^*)$, the bootstrap estimator of $r_{\hat{P}_n}^{\theta,k}(\boldsymbol{\theta}_0)$ is

$$\hat{r}_{\hat{P}_n}^{\theta,k}(\boldsymbol{\theta}_0) = \frac{\#\{\theta_i^* : \mathrm{D}_\theta(\theta_i^*;\hat{P}_n) \leq \mathrm{D}_\theta(\boldsymbol{\theta}_0;\hat{P}_n)\}}{N}\,. \tag{11}$$

Remark 2.1. A similar notion to (10), built for the sample mean of a number of consecutive observations, and called *relative rank* was defined in [29] to build data depth based moving-average control charts. Also [15] considered a notion somewhat related to (11) when they studied the (data) depth-based rank of an element of a parameter space with respect to a sample of bootstrap estimates of the parameter.

In our setting, the element $\boldsymbol{\theta}_0$ of the parameter space to be ranked is the estimate obtained at a given sample. In such a case we can reformulate (9) using a sample instead of an element of the parameter space as argument and talk about the rank of the sample with regard to θ,

$$r_P^{\theta}(\boldsymbol{x}^{(k)}) = r_P^{\theta,k}(\hat{\theta}(\boldsymbol{x}^{(k)})) = \Pr\{Y^{(k)} : \mathrm{D}_\theta(\hat{\theta}(Y^{(k)});P) \leq \mathrm{D}_\theta(\hat{\theta}(\boldsymbol{x}^{(k)});P)\}\,,$$

where $\boldsymbol{x}^{(k)} = (\boldsymbol{x}_1,\ldots,\boldsymbol{x}_k)$ and $Y^{(k)}$ is a random sample of P of size k. Notice that the superindex referring to the sample size k is omitted from the notation because it is reflected on the argument of the rank function.

Theorem 2.1. *If $X^{(k)} = (X_1,\ldots,X_k)$ is a random sample drawn from a continuous distribution P and $\mathrm{D}_\theta(\hat{\theta}(X^{(k)});P)$ is a continuous random variable, then*

1. *$r_P^{\theta}(X^{(k)})$ is uniformly distributed in the unit interval.*
2. *if further the empirical θ-depth is uniformly consistent as an estimator of D_θ, then for any $\boldsymbol{\theta}_0$ it holds that $r_{\hat{P}_n}^{\theta,k}(\boldsymbol{\theta}_0) \longrightarrow_n r_P^{\theta,k}(\boldsymbol{\theta}_0)$ a.s.*

3. *under the conditions of 2.,* $r^{\theta}_{\hat{P}_n}(X^{(k)})$ *converges weakly to a uniform distribution in the unit interval.*

Proof. 1. follows from the probability distribution transformation. Clearly $r^{\theta,k}_{P}(\boldsymbol{\theta}_0)$ is the cdf of the random variable $\mathrm{D}_\theta(\hat{\theta}(X^{(k)}); P)$, with $X^{(k)}$ a random sample of P of size k, evaluated at $\mathrm{D}_\theta(\boldsymbol{\theta}_0; P)$. Consequently, as long as $\mathrm{D}_\theta(\hat{\theta}(X^{(k)}); P)$ is a continuous random variable, the rank $r^{\theta}_{P}(X^{(k)})$ is uniformly distributed in the unit interval.

2. follows from the uniform consistency of D_θ. Consider a sequence of empirical distributions such that $\sup_{\boldsymbol{\theta}_0} |\mathrm{D}_\theta(\boldsymbol{\theta}_0; \hat{P}_n) - \mathrm{D}_\theta(\boldsymbol{\theta}_0; P)| \longrightarrow_n 0$. For any $\varepsilon > 0$ and for n large enough,

$$\begin{aligned}\{Y^{(k)} : \mathrm{D}_\theta(\hat{\theta}(Y^{(k)}); P) \leq \mathrm{D}_\theta(\boldsymbol{\theta}_0; P) - \varepsilon\} \subset \{Y^{(k)} : \mathrm{D}_\theta(\hat{\theta}(Y^{(k)}); \hat{P}_n) \leq \mathrm{D}_\theta(\boldsymbol{\theta}_0; \hat{P}_n)\} \\ \subset \{Y^{(k)} : \mathrm{D}_\theta(\hat{\theta}(Y^{(k)}); P) \leq \mathrm{D}_\theta(\boldsymbol{\theta}_0; P) + \varepsilon\}\,,\end{aligned}$$

so the result is proved by letting ε tend to 0.

3. is straightforward after *1.* and *2.* □

Corollary 2.1. *If P is continuous and $X^{(k)}$ is a random sample of P of size k, any of the following random variables is uniformly distributed in the unit interval*

1. $r^{\mu}_{P}(X^{(k)}) = \Pr\{Y^{(k)} : \mathrm{D}_\mu(\overline{Y}; P) \leq \mathrm{D}_\mu(\overline{X}; P)\}$;
2. $r^{\sigma}_{P}(X^{(k)}) = \Pr\{Y^{(k)} : \mathrm{D}_\sigma(S_k(Y^{(k)}); P) \leq \mathrm{D}_\sigma(S_k(X^{(k)}); P)\}$;
3. $r^{(\mu,\sigma)}_{P}(X^{(k)}) = \Pr\{Y^{(k)} : \mathrm{D}_{\mu,\sigma}((\overline{Y}, S_k(Y^{(k)})); P) \leq \mathrm{D}_{\mu,\sigma}((\overline{X}, S_k(X^{(k)})); P)\}\,,$

where $Y^{(k)}$ is a random sample of P of size k. Further, both of $r^{\mu}_{\hat{P}_n}(X^{(k)})$ and $r^{(\mu,\sigma)}_{\hat{P}_n}(X^{(k)})$ converge weakly to a uniform distribution in the unit interval.

3. Nonparametric depth and rank charts

Consider a quality characteristic and a sample of observations of it, $x_1, \ldots, x_n$, which we will hereafter refer to as *historical dataset*. We will now explain how to obtain the control limits of the new charts from the historical dataset and how to polish it, in case it is needed. In Statistical Process Control jargon these tasks are referred to as Phase I, while the usage of the charts to detect departures from a prescribed distribution is Phase II.

In brief, for a given notion of parameter depth and an estimator of the parameter based on samples of size k, we take a sufficiently large number of subsamples of size k by resampling from the historical dataset. For each of these subsamples, we estimate the parameter and determine the parameter depth of such estimation with respect to the historical dataset. Finally, we take the α-quantile of the sample of parameter depths for the desired false alarm rate α as a control limit and use it on future samples.

3.1. Building of the final chart

In first place, the size k of the samples that will be taken and the parameter of the quality characteristic to consider θ is decided. In case the estimator of the parameter $\hat{\theta}$ is different from the plug-in one, it should be specified. Also the false alarm rate α must be fixed. The next three steps explain how to build a D-chart (1. to 3.D) and the corresponding r-chart (1. to 3.r).

1. Within the n historical observations take, at random, a sample of size k, $X_1^*, \ldots, X_k^*$, compute $\hat{\theta}(X_1^*, \ldots, X_k^*)$, and determine its θ-depth with respect to the historical dataset.

2. Repeat the previous step a large number of times and determine the α-quantile of all obtained θ-depths, denoted by d_α.

3.D The control limit of a D-chart is set at d_α. The D-chart is used to represent the θ-depths of estimates of the parameter obtained over future samples of size k and only θ-depths not below d_α are allowed in the in-control state.

3.r The control limit of an r-chart is set at α. For each new sample, compute the θ-depth of the estimation of θ over it and represent at the r-chart the fraction of θ-depths from 2. that are below the new θ-depth.

3.2. Polishing historical data

Commonly the historical dataset consists of m trial samples of size k each ($n = mk$) and the false alarm probability is set at $\alpha = 0.0027$. For such a small α, it is possible to use the control charts to polish the historical dataset by getting rid of any trial sample that is suspected to have been obtained when an assignable cause was present.

2.1 Check that none of the θ-depths of a trial sample is below d_α. In case some is, study the presence of some assignable cause when it was taken and delete it if such presence is confirmed. In case the trial samples cannot be traced and some of their θ-depths is below d_α, we suggest to delete such samples under the assumption that they were taken when the process was out-of-control. If some trial sample is deleted, repeat 2. with the remaining trial samples until none of their θ-depths is below d_α.

D-*charts vs.* r-*charts.* If the estimate of θ on a generic sample of the production is denoted by $\hat{\theta}$, a depth D-chart tracks the evolution of $\mathrm{D}_\theta(\hat{\theta}; \hat{P}_n)$ with the control limit set at d_α, while a rank r-chart tracks the evolution of $\hat{r}_{\hat{P}_n}^{\theta,k}(\hat{\theta})$ with the control limit set at α. Nevertheless, both charts will lead to the same conclusions. Obviously in the very special case that the distribution of the quality characteristic, P, is completely known, the computation of d_α would be done with regard to it (as in Section 4 with the normal distribution) and either of $\mathrm{D}_\theta(\hat{\theta}; P)$ or $r_P^{\theta,k}(\hat{\theta})$ are tracked.

4. Normal depth charts

Under the assumption that P follows a given distribution, for example a normal one, and for any $\alpha \in (0,1)$, we can determine the depth level d such that

$$\Pr\left(\hat{\theta}(X^{(k)}) \in \mathrm{D}_\theta^d(P)\right) = 1-\alpha\,,$$

where $X^{(k)} = (X_1, \ldots, X_k)$ is a random sample of P of size k. We are particularly concerned with the parameters μ, σ, and (μ,σ) of a normal distribution with respective plug-in estimators $\overline{X}$, S_k, and $(\overline{X}, S_k)$. Due to the equivariance properties of the μ-, σ- and (μ,σ)-depths and the fact that the normal distribution is closed under affine transformations, the trimming level d_α that serves as control limit for either of such parameter depths does not depend on the specific Gaussian distribution in consideration. We would like to point out that despite we have the exact (theoretical) control limit, the polishing of the historical dataset as described in Section 3.2 is highly recommendable in real applications.

The consistency of the parameter depth-trimmed regions shown at (3) supports the usage of d_α as control limit of a D-chart since it establishes that, whenever enough historical data are available, we can use the empirical trimmed regions as reasonable approximations of the population ones.

4.1. Normal depth chart for $\overline{X}$

Given a univariate standard normal probability distribution, its μ-trimmed region of level d is the closed interval $[-r_d, r_d]$, where

$$r_d = \frac{\exp\{-z_d^2/2\}}{d\sqrt{2\pi}}\,,$$

which can be obtained after immediate application of (2), see also [23, Ex. 3, Sec. 6].

The equivariance of the μ-trimmed regions presented in Section 2 guarantees that $\mathrm{D}_\mu^d(\langle X, \boldsymbol{u}\rangle) = \{\langle \boldsymbol{x}, \boldsymbol{u}\rangle : \boldsymbol{x} \in \mathrm{D}_\mu^d(P_X)\}$ for all $\boldsymbol{u} \in \mathbb{R}^p$ and therefore the μ-depth-trimmed region of level d of a p-dimensional standard normal probability distribution P is the closed ball centred at the origin with radius r_d, that is, $\mathrm{D}_\mu^d(P) = B(r_d)$.

Finally, we denote by $s_{\alpha,k,p}$ the radius of the closed ball centred at the origin that contains the sample mean of a sample of k p-dimensional standard normal random vectors, $\overline{X}$, with probability $1-\alpha$. Clearly $s_{\alpha,k,p}$ is given by

$$\Pr\left(\overline{X} \in B(s_{\alpha,k,p})\right) = 1-\alpha\,, \quad \text{where } s_{\alpha,k,p} = \sqrt{\chi^2_{p,\alpha}/k}\,.$$

For any dimension p, and any false alarm probability α, it is possible to determine the depth d such that $r_d = s_{\alpha,k,p}$. After the affine equivariance of the μ-depth, the relation between d and α holds true for any p-dimensional normal probability distribution. The solutions to the equation $r_d = s_{\alpha,k,p}$ for sample sizes $k = 1, \ldots, 15$, values of α equal to 0.5, 0.1, 0.05, 0.01, and 0.0027, and dimensions $p = 1, \ldots, 6$ are presented in Table 5 (see the Appendix) and serve as control limits of the D_μ-chart.

4.2. Normal depth chart for S

The σ-trimmed region of level d of a univariate standard normal probability distribution P is the closed interval given below

$$\mathrm{D}^d_\sigma(P) = \left[\sqrt{1 - \frac{2z_{(1-d)/2}}{d\sqrt{2\pi}} \exp\left\{-z^2_{(1-d)/2}/2\right\}}, \sqrt{1 + \frac{2z_{d/2}}{d\sqrt{2\pi}} \exp\left\{-z^2_{d/2}/2\right\}}\right] .$$

Such an interval does also correspond to the values that are the square root of $\mathrm{D}_\mu(P_{X^2})$, where X is a univariate standard normal random variable. The identity of the upper extremes is obvious, while the one of the lower extremes can be shown after standard optimization procedures. See Figure 1 for the σ-regions of a standard normal variable at any level d.

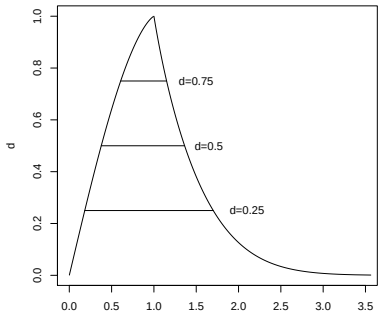

Figure 1: σ-regions of a standard Gaussian distribution.

Since kS^2_k follows a chi-square distribution with $k-1$ degrees of freedom, the probability content of $\mathrm{D}^d_\sigma(P)$ for random variable S_k is

$$\Pr(S_k \in \mathrm{D}^d_\sigma(P)) = F_{\chi^2_{k-1}}\left(k + k\frac{2z_{d/2}}{d\sqrt{2\pi}} \exp\left\{-z^2_{d/2}/2\right\}\right) - F_{\chi^2_{k-1}}\left(k - k\frac{2z_{(1-d)/2}}{d\sqrt{2\pi}} \exp\left\{-z^2_{(1-d)/2}/2\right\}\right) ,$$

where $F_{\chi^2_{k-1}}$ is the cdf of a chi-square distribution with $k-1$ degrees of freedom.

For any fixed value of α, we can solve the equation $\Pr(S_k \in \mathrm{D}^d_\sigma(P)) = 1-\alpha$ in order to obtain the control limit of the D_σ-chart. Table 6 shows the corresponding values of d for α equal to 0.5, 0.1, 0.05, 0.01, 0.0027, and sample sizes $k = 2, \ldots, 15$.

4.3. Normal depth chart for $(\overline{X}, S)$

Consider a sample of k observations of a univariate standard normal probability distribution P and follow the standard notation to represent the sample mean of squares by $\overline{X^2}$. We have

$$\Pr\left((\overline{X}, S_k) \in \mathrm{D}^d_{(\mu,\sigma)}(P)\right) = \Pr\left((\overline{X}, \overline{X^2}) \in \mathrm{D}^d_\mu(P_{(X,X^2)})\right) . \tag{12}$$

It is thus crucial to determine the boundary of the compact set $\mathrm{D}_\mu^d(P_{(X,X^2)})$, where X is a standard normal random variable, in order to be able to compute the probability presented in (12).

For each $d \in (0,1]$, the boundary of $\mathrm{D}_\mu^d(P_{(X,X^2)})$ can be parametrized as $\{(x(d,t), y(d,t)) : t \in [0,1]\}$ with

$$x(d,t) = \frac{1}{d}\int_{\Phi^{-1}(t)}^{\Phi^{-1}(t+d)} x\phi(x)\mathrm{d}x = \frac{1}{d}\left(\phi(\Phi^{-1}(t)) - \phi(\Phi^{-1}(t+d))\right)$$
$$y(d,t) = \frac{1}{d}\int_{\Phi^{-1}(t)}^{\Phi^{-1}(t+d)} x^2\phi(x)\mathrm{d}x = 1 + \frac{1}{d}\left(\Phi^{-1}(t)\phi(\Phi^{-1}(t)) - \Phi^{-1}(t+d)\phi(\Phi^{-1}(t+d))\right)$$

if $t \in [0, 1-d]$, and

$$x(d,t) = \frac{1}{d}\left(\int_{-\infty}^{\Phi^{-1}(t+d-1)} x\phi(x)\mathrm{d}x + \int_{\Phi^{-1}(t)}^{+\infty} x\phi(x)\mathrm{d}x\right) = \frac{1}{d}\left(\phi(\Phi^{-1}(t)) - \phi(\Phi^{-1}(t+d-1))\right)$$
$$\begin{aligned} y(d,t) &= \frac{1}{d}\left(\int_{-\infty}^{\Phi^{-1}(t+d-1)} x^2\phi(x)\mathrm{d}x + \int_{\Phi^{-1}(t)}^{+\infty} x^2\phi(x)\mathrm{d}x\right) \\ &= 1 + \frac{1}{d}\left(\Phi^{-1}(t)\phi(\Phi^{-1}(t)) - \Phi^{-1}(t+d-1)\phi(\Phi^{-1}(t+d-1))\right), \end{aligned}$$

if $t \in (1-d, 1]$, where ϕ stands for the density mass function of the standard normal, Φ for its cdf, and Φ^{-1} for its quantile function. See Figure 2 for the contours of the (μ,σ)-regions of a standard normal variable X as well as those of the zonoid regions of (X, X^2) at some prescribed levels.

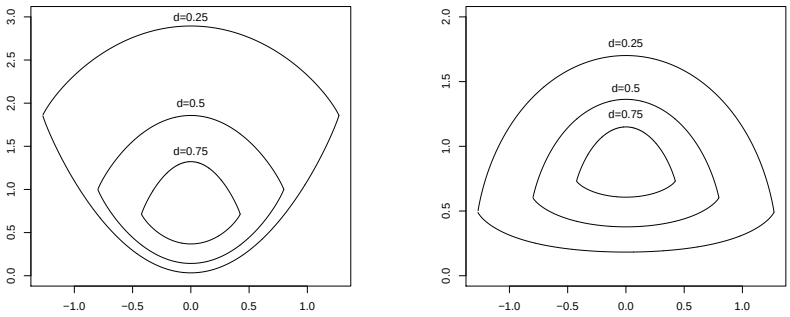

Figure 2: Contours of the zonoid (μ)-regions of (X, X^2), where X follows standard normal distribution (left) and contours of the (μ,σ)-regions of a standard normal random variable (right).

Since the random vector $(\overline{X}, \overline{X^2})$ is a transformation of $(\overline{X}, S_k^2)$ whose distribution is known, it is possible to integrate numerically over $\mathrm{D}_\mu^d(P_{(X,X^2)})$ in order to obtain its probability content. We can also compute the (μ,σ)-depth of (m,s) with respect to a standard normal distribution solving the system of nonlinear equations $x(d,t) = m$ and $y(d,t) = s^2 + m^2$ in terms of d (and t).

Table 7 shows the values of d that correspond to α equal to 0.5, 0.1, 0.05, 0.01, 0.0054, and 0.0027 for sample sizes $k = 2, \ldots, 10$. These values serve as the control limit of the $\mathrm{D}_{(\mu,\sigma)}$-chart. The control limits corresponding to $k \geq 5$ have been obtained by numerical integration over $\mathrm{D}_{\mu}^{d}(P_{(X,X^2)})$, while those corresponding to $k < 5$ have been approximated as the quantiles of a sample of 10^6 (μ, σ)-depths.

Since the variability of X^2 is greater than the one of X, it is often convenient to downweight the estimator of the sample standard deviation and use the standard deviation of the historical dataset as reference value. In order to do so, we estimate (μ, σ) by $(\overline{X}, \sqrt{\delta S_k^2 + (1-\delta)\sigma_0^2})$ for some weight $0 \leq \delta \leq 1$, where σ_0 is the in-control standard deviation. In the standardized case $\sigma_0 = 1$ and when working with real data, σ_0 is estimated form the historical dataset as its sample standard deviation denoted by $\hat{\sigma}_0$. Formula (12) turns now into

$$\Pr\left(\left(\overline{X}, \sqrt{\delta S_k^2 + 1 - \delta}\right) \in \mathrm{D}_{(\mu,\sigma)}^{d}(P)\right) = \Pr\left((\overline{X}, \delta\overline{X^2} + (1-\delta)(\overline{X}^2 + 1)) \in \mathrm{D}_{\mu}^{d}(P_{(X,X^2)})\right).$$

A reasonable value for δ is 0.5, which is below the ratio of the standard deviations of X and X^2 (specifically $1/\sqrt{2}$) in order to reflect the more relevant role of the mean with respect to the standard deviation in statistical quality control. Table 8 shows the values of d that correspond to α equal to 0.5, 0.1, 0.05, 0.01, 0.0054, and 0.0027 for sample sizes $k = 2, \ldots, 10$ when $\delta = 0.5$.

5. Examples and applications

In the current section we present five examples and applications. The first application is based on real data and contains Phase I and Phase II for D_{μ}, D_{σ}, and $\mathrm{D}_{(\mu,\sigma)}$. The remaining four cases of study are based on simulated data with $\alpha = 0.05$ and only Phase I (without polishing due to the synthetic nature of the data) is considered at them.

5.1. Univariate Gaussian (piston rings)

Consider the classical dataset on piston ring diameters provided in [8, Tables 6.3 and 6E.7]. This dataset consists of 40 samples of $k = 5$ piston ring diameters each. The first 25 samples are the trial ones, that is the historical dataset consists of $n = 25 \times 5 = 125$ observations which are used to obtain the control limits (Phase I). We cannot reject that this historical dataset is normally distributed (p-value= 0.89093 at the Shapiro-Wilk normality test), so we will use the control limits given at Tables 5, 6, 7, and 8.

Location, D_{μ}*-chart.* The sample means of the piston ring diameters are monitored by means of the D_{μ}-chart with control limit $d = 0.22163$ obtained from Table 5 ($p = 1$, $k = 5$, $\alpha = 0.0027$). In Figure 3 left, the first 25 points correspond to the sample means of the 25 trial samples, the dashed center line is established at the average diameter of the historical dataset and the control limits (solid lines) are presented at the extreme values of $\mathrm{D}_{\mu}^{d}(\hat{P}_n)$ for $d = 0.22163$, where $\hat{P}_n$ is the empirical distribution associated with the historical dataset. In fact, these control limits (essentially) coincide with the the ones of the Shewart $\overline{X}$-chart with the classical $\pm 3\sigma$ rule, see Table 1. In Figure 3

right, the first 25 points correspond to the μ-depths of the sample means of the 25 trial samples with regard to the historical dataset, while the control limit (solid line) is set at $d = 0.22163$ and the dashed line is the trimming level that corresponds to $\alpha = 0.5$. In either of the two charts, the sample means of all 25 trial samples are inside the control region and there is no reason to exclude any of them. In order to finish Phase I, we should depict a variability control chart (e.g. the S-chart) in order to check that the trial samples were taken with the process in the in-control state. As seen in Figure 4, which will be discussed in detail later on, there is no reason to suspect that an assignable cause affects any of the trial samples.

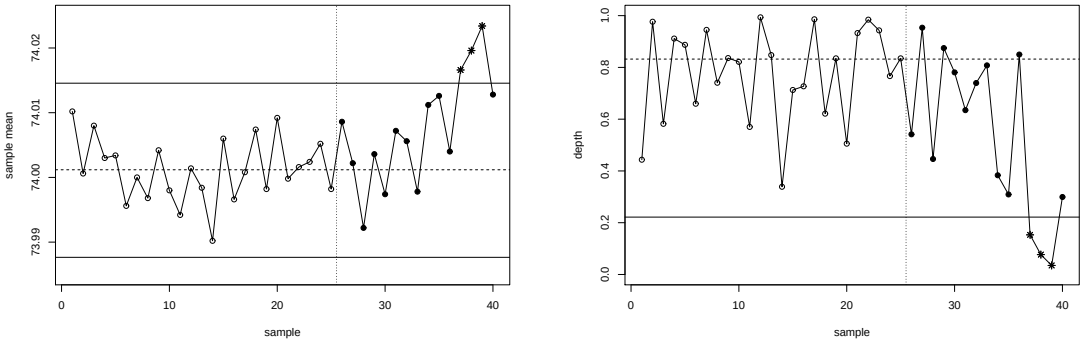

Figure 3: $\overline{X}$-chart based on the μ-depth (left) and D_μ-chart (right).

	Shewhart $\overline{X}$-chart	$\mathrm{D}_\mu^d(\hat{P}_n)$
UCL	74.01444	74.01456
LCL	73.98791	73.98765

Table 1: Comparison of Upper and Lower Control Limits of Shewhart $\overline{X}$-chart and D_μ-chart.

In Phase II, the control charts are used to monitor the sample means of 15 new samples, which are represented by bullets if they lie in the in-control region, while they are represented by stars when they are out-of-control. From either of the two charts, we conclude that samples #37, #38, and #39 were taken with the process in the out-of-control state.

In case the normality of the historical dataset would have been rejected, we would need to resample from it in order to estimate the trimming level d that corresponds to $\alpha = 0.0027$. We have run such experiment, and after resampling 10000 times, we obtained $d = 0.21338$, which leads to the same conclusions as the normal trimming level.

Scale, D_σ*-chart.* The sample standard deviations of the piston ring diameters are monitored by means of the chi-square based S-chart [8, Sec. 6.3.3] and the D_σ-chart with control limit $d = 0.17922$ obtained from Table 6 ($k = 5$, $\alpha = 0.0027$).

In Figure 4 left, the first 25 points correspond to the sample standard deviations of the 25 trial samples, while the dotted lines correspond to the control limits of the chi-square based S-chart ($\alpha = 0.0027$) and the solid lines to the extremes of $\mathrm{D}^d_\sigma(\hat{P}_n)$, that is, the σ-depth control region. In Figure 4 right, the first 25 points correspond to the σ-depths of the sample standard deviations of the 25 trial samples with regard to the historical dataset, while the control limit is set at $d = 0.17922$. In either of the two charts, the sample standard deviations of all 25 trial samples are within the control region and there is no reason to exclude any of them. At this point we should make clear that, despite of the presentation provided here, Phase I of location and scale charts are designed to be done simultaneously.

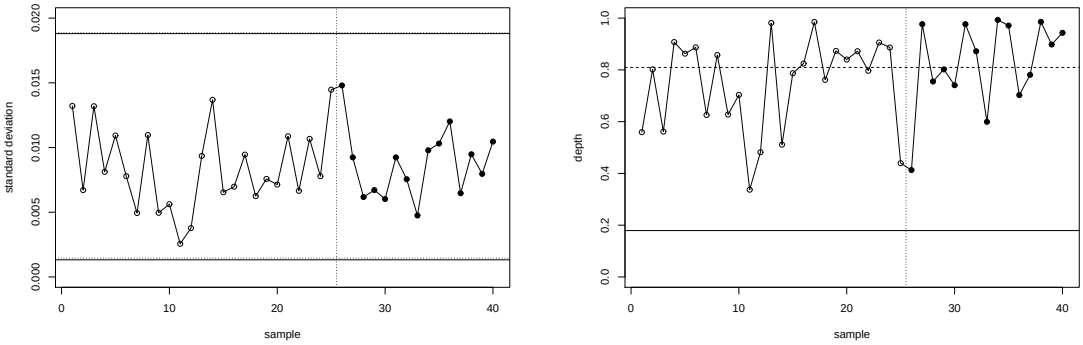

Figure 4: S-chart based on the σ-depth of S_k (left) and D_σ-chart (right).

In Phase II, the control charts are used to monitor the sample standard deviations of 15 new samples, which are represented by bullets in the charts. All sample standard deviations fall within the control region.

Location-scale, $\mathrm{D}_{(\mu,\sigma)}$*-charts.* The bivariate statistic $(\overline{X}, \sqrt{\delta S_k^2 + (1-\delta)\hat{\sigma}_0^2})$ evaluated on each sample of piston ring diameters is monitored by means of a $\mathrm{D}_{(\mu,\sigma)}$-chart. We have modified the false alarm probability with regard to the one used to monitor the location and the scale, since the previous charts are conceived to be used in combination, while this one is to be used on its own. After Bonferroni correction, the current chart will be built for false alarm rate $\alpha = 2 \times 0.0027 = 0.0054$ in order to be comparable with the previous ones.

In Figure 5 top left, we have considered $\delta = 1$, so the 25 white circles correspond to the statistic $(\overline{X}, S_k)$ of each of the 25 trial samples, while the solid line is the contour of the (μ, σ)-region with respect to the historical dataset, $\mathrm{D}^d_{(\mu,\sigma)}(\hat{P}_n)$ with $d = 0.14873$ (see Table 7, $k = 5$, $\alpha = 0.0054$). In Figure 5 top right, the first 25 points correspond to the (μ, σ)-depths of the sample standard deviations of the 25 trial samples with regard to the historical dataset, while the control limit is set at $d = 0.14873$. In either of the two charts, all white circles lie within the control region, so none of the trial samples is excluded and Phase I is concluded. Observe that Phase I involves here the

usage of a single control chart.

The bottom charts in Figure 5 are equivalent to the ones on top, but now the used statistic is $(\overline{X}, \sqrt{\delta S_k^2 + (1-\delta)\hat{\sigma}_0^2})$ with $\delta = 0.5$, so $d = 0.19233$, see Table 8, $k = 5$, $\alpha = 0.0054$.

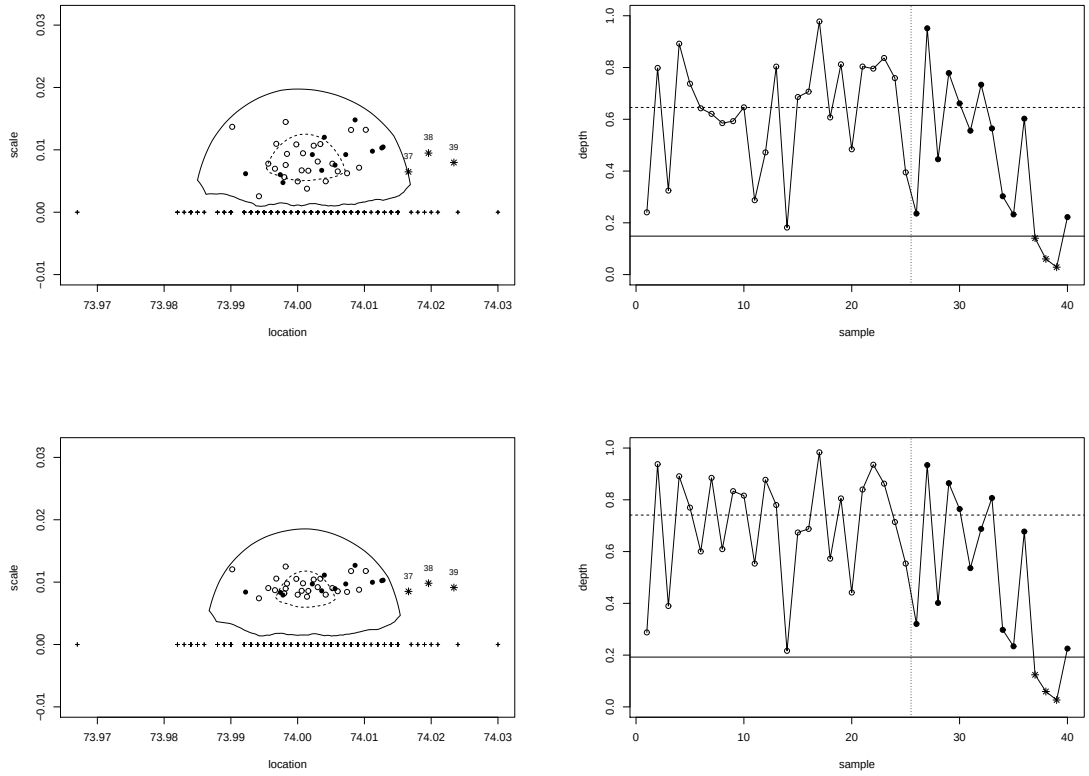

Figure 5: $D_{(\mu,\sigma)}$-charts (right) and corresponding regions (left) for $\delta = 1$ (top) and $\delta = 0.5$ (bottom).

In Phase II, the control charts are used to monitor $(\overline{X}, \sqrt{\delta S_k^2 + (1-\delta)\hat{\sigma}_0^2})$ on 15 new samples, which are represented by bullets if in-control and stars if out-of-control. As in the $\overline{X}$-chart, we conclude that samples #37, #38, and #39 are out-of-control.

5.2. Univariate Exponential

In order to present an application of our D_μ-chart with nongaussian data, we reproduce the exponential part of Simulation Example A in [30]. A random sample of size $n = 100$ is drawn from an Exponential distribution with $\lambda = 1$ and a subgroup is formed for each $k = 4$ consecutive observations (25 trial samples).

The control limits of several control charts for the mean of samples of size $k = 4$ are presented in Table 2. These charts are either theoretical or built from the same $100 = 25 \times 4$ historical

observations and out of the same 200 bootstrap samples of size $k = 4$ taken from them whenever needed. The 200 bootstrap sample means were used to obtain bootstrap estimates of the control limits of the $\overline{X}$-chart (with $\alpha = 0.1$, 0.05, and 0.02) as proposed by Liu and Tang [30]. Notice that the depth-based procedure proposed by Liu and Singh [15] applied with the halfspace or simplicial depth would lead to the same control limits. The exact trimming level d for the D_μ-chart for exponential data is presented together with the exact control limits, and the trimming level d estimated from the 200 bootstrap samples is presented together with the estimated control limits. The control limits (exact and estimated) obtained under assumption of normality together with the trimming level d obtained from Table 5 are also presented.

α	0.1	0.05	0.02
Control chart	LCL ; UCL	LCL ; UCL	LCL ; UCL
exact two-sided test	0.342 ; 1.938	0.273 ; 2.192	0.206 ; 2.511
Liu and Tang [30], Liu and Singh [15]	0.347 ; 2.06	0.278 ; 2.267	0.237 ; 2.641
exact μ-depth	0.273 ; 1.787	0.207 ; 2.022	0.146 ; 2.328
exponential	($d = 0.455$)	($d = 0.36$)	($d = 0.265$)
simulated μ-depth	0.256 ; 1.879	0.188 ; 2.074	0.113 ; 2.453
no distribution assumption	($d = 0.4214576$)	($d = 0.34561$)	($d = 0.2353238$)
exact μ-depth	0.295 ; 1.724	0.228 ; 1.936	0.167 ; 2.211
Gaussianity assumed	($d = 0.48472$)	($d = 0.39211$)	($d = 0.29802$)
simulated μ-depth	0.315 ; 1.745	0.227 ; 1.948	0.17 ; 2.283
Gaussianity assumed	($d = 0.48472$)	($d = 0.39211$)	($d = 0.29802$)

Table 2: Several $\overline{X}$-charts for exponential data.

In Figure 6 top, the $\overline{X}$-chart ($\alpha = 0.05$) for the 25 trial samples of size $k = 4$ is presented. The solid lines correspond to the extreme values of $D_\mu^d(\hat{P}_n)$ for the estimated trimming level d (tag 'no distribution assumption' in Table 2), the dashed lines to the extreme values of $D_\mu^d(\hat{P}_n)$ when d is obtained from Table 5 (tag 'Gaussianity assumed' in Table 2), while the dotted lines are the bootstrap control limits (tag 'Liu and Tang [30], Liu and Singh [15]' in Table 2). In either case samples #13 and #17 are out-of-control. In Figure 6 bottom, a depth chart with the estimated D_μ control limit (solid line) and Gaussian control limit (dashed line) is presented, while the corresponding r-chart is presented on the right.

5.3. Bivariate Gaussian

We have simulated 40 samples of $k = 5$ observations of a standard bivariate normal random vector. Figure 7 right represents the D_μ-chart for $\alpha = 0.05$. The control limit is set at trimming level $d = 0.33138$ (see Table 5, $p = 2$, $\alpha = 0.05$, $k = 5$). In order to check the stability of this control limit we obtained 2000 bootstrap samples of size $k = 5$ for the historical dataset and the estimation of the trimming level was 0.3326941.

In Figure 7 left, the contour of the (zonoid) trimmed region $D_\mu^d(\hat{P}_n)$ is plotted with a solid line, while the (almost coincident) dotted line represents an ellipse that corresponds to the in-control

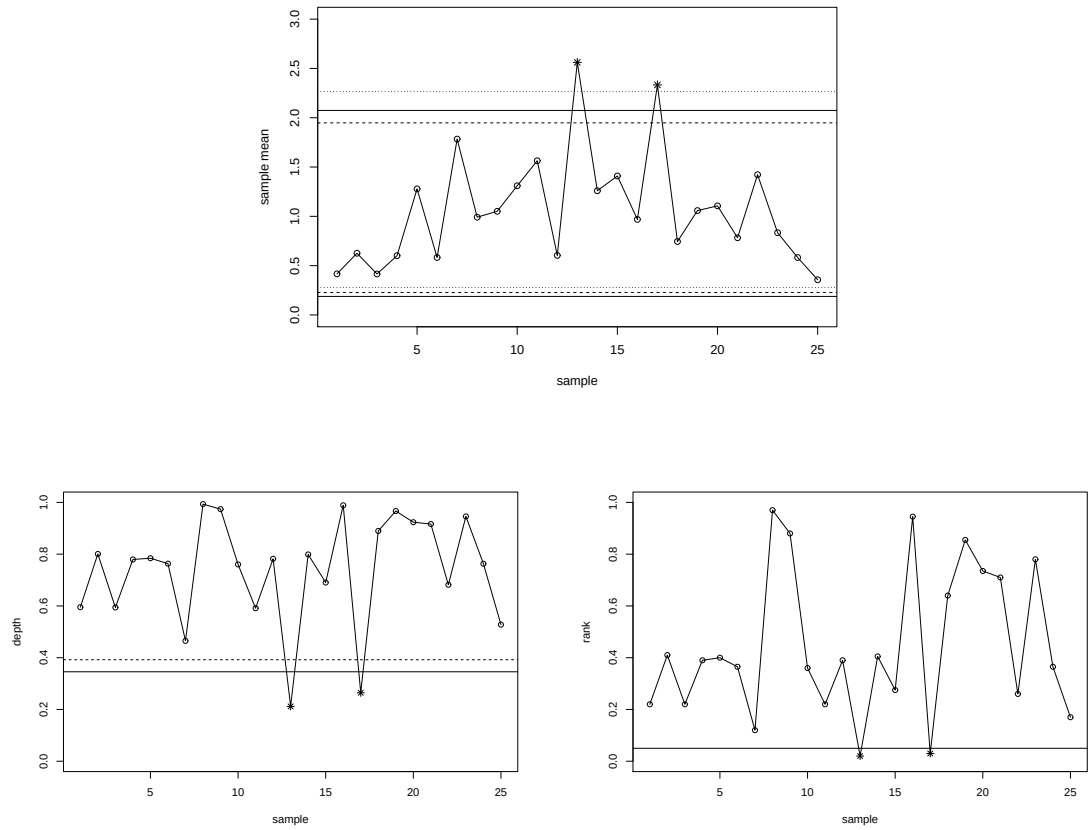

Figure 6: $\overline{X}$-chart for Exponential data (top) and D_μ-chart (bottom left) together with corresponding r-chart (bottom right).

region of the Hotelling T^2-chart, see [8, Sec. 11.3]. Observations are presented by dots and sample means by either circles or stars depending on whether they lie inside or outside the in-control region.

5.4. Bivariate Skew Normal

We have simulated 60 samples of $k = 3$ observations of a bivariate random vector with Skew Normal distribution, see [31], with parameters $\xi = (0.5, -1)$, $\Omega = \begin{pmatrix} 1 & 0.8 \\ 0.8 & 2 \end{pmatrix}$, and $\alpha = (10, 10)$. From this historical dataset (180 bivariate observations), we have taken 10000 bootstrap samples of size $k = 3$ and obtained a trimming level $d = 0.19$ as control limit for the D_μ-chart with $\alpha = 0.05$. The control limit under Gaussianity ($p = 2$, $\alpha = 0.05$, $k = 4$) is 0.19524, see Table 5. Figure 8 bottom left represents the D_μ-chart obtained, the solid line is the estimated control limit. The dashed line is the Gaussian control limit, on the right the corresponding r-chart is presented on the right.

In Figure 8 top, the contour of the (zonoid) trimmed region $\mathrm{D}_\mu^d(\hat{P}_n)$ with the estimated trimming

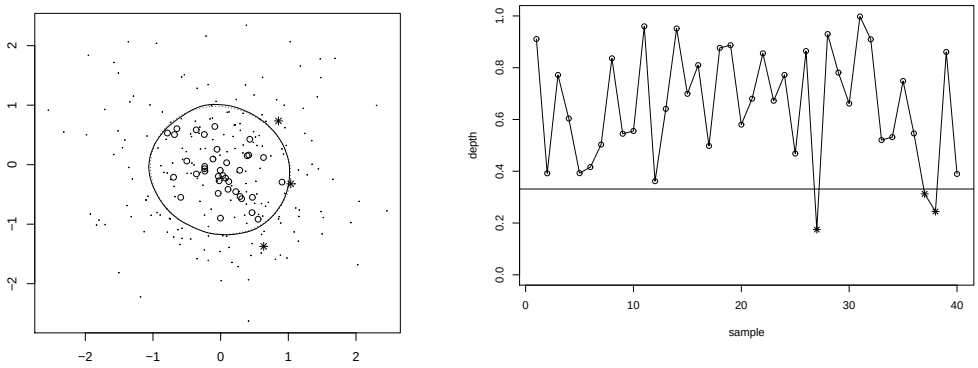

Figure 7: D_μ-chart for bivariate Gaussian data (right) and corresponding region (left).

is plotted with a solid line, with the Gaussian trimming level with a dashed line, while the dotted line represents an ellipse that corresponds to the in-control region of the Hotelling T^2-chart, which always assumes Gaussianity. Observe that the T^2-chart detects one more out-of-control sample that our chart and its in-control region (for averages of samples of size 3) contains some points out of the convex hull of the historical dataset.

A modification of the T^2-chart for skewed populations by means of weighted standard deviation has been proposed in [13]. The in-control region of this modified T^2-chart consists in an ellipse that is dilated by a different scale factor at each or the orthants with vertex on the mean of the historical dataset. This means, among other things, that the contour of the in-control region is not smooth and it can be affected by rotations of the dataset.

5.5. Bivariate Exponential

We have simulated 50 samples of $k = 4$ observations of a bivariate random vector with independent Exponential marginal distributions with rate $\lambda = 1$ each. From this historical dataset (200 bivariate observations), we have taken 2000 bootstrap samples of size $k = 4$ and obtained a trimming level $d = 0.239155$ as control limit for the D_μ-chart with $\alpha = 0.05$. The control limit under Gaussianity ($p = 2$, $\alpha = 0.05$, $k = 4$) is 0.27033, see Table 5. Figure 9 bottom left represents the D_μ-chart obtained, the solid line is the estimated control limit, while the dashed line is the Gaussian control limit, on the right the corresponding r-chart is presented.

In Figure 9 top, the contour of the (zonoid) trimmed region $D^d_\mu(\hat{P}_n)$ with the estimated trimming is plotted with a solid line, with the Gaussian trimming level with a dashed line, while the dotted line represents an ellipse that corresponds to the in-control region of the Hotelling T^2-chart, which always assumes Gaussianity.

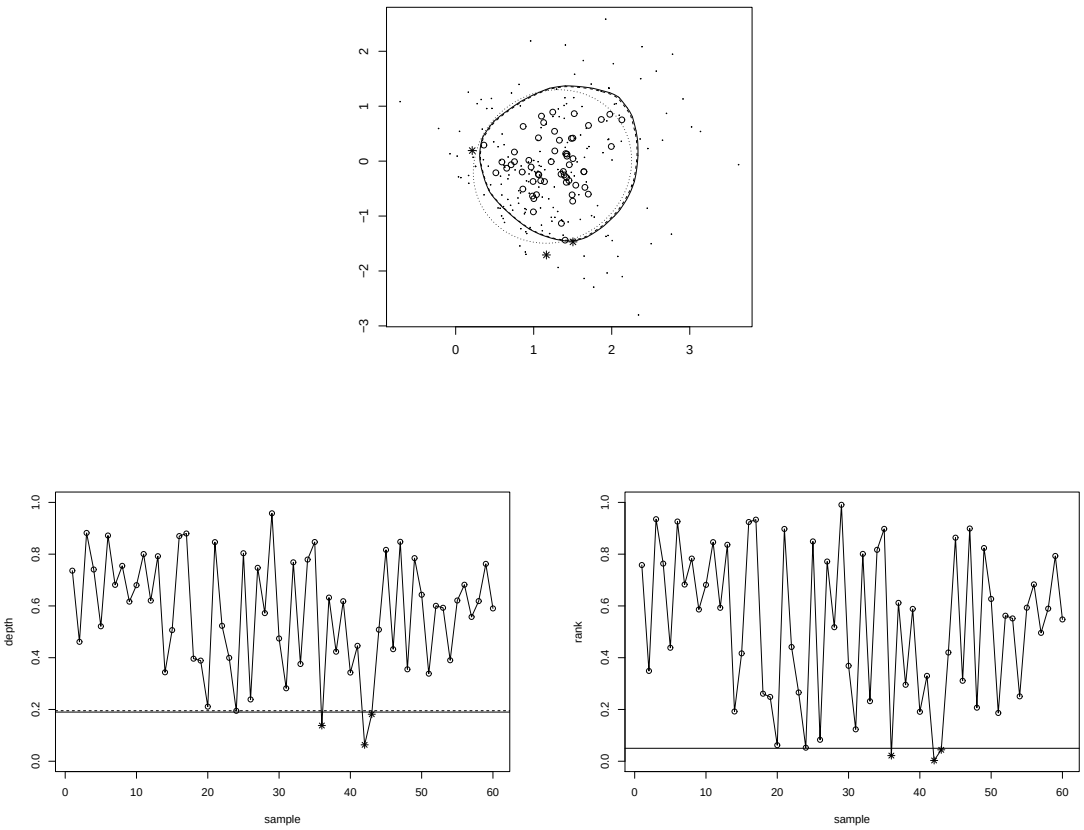

Figure 8: D_μ-chat and r-chart for bivariate Skew Normal data (bottom) with corresponding region (top).

6. Comparison of OC curves and ARLs

Throughout the current section, we use numerical integration techniques to compare the asymptotic performance of the new D-charts under the assumption of normality with other classical control charts by means of both the Operating Characteristic (OC) curves (Secs. 6.1, 6.2, and 6.3) and the Average Run Length (ARL) until a shift is detected (Sec. 6.4). The performance of the $D_{(\mu,\sigma)}$-chart when the historical dataset is small will be compared by means of simulations with several other control charts for joint monitorization of location and scale (Sec. 6.5).

An OC curve depicts the probability that a given shift in the prescribed distribution of the quality characteristic is not detected in a control chart versus the magnitude of the given shift. Control charts, specially when used in Phase II applications, are often identified with statistical hypothesis tests. The null hypothesis establishes that the process follows a prescribed distribution, the alternative that there has been a shift on the distribution, and the false alarm rate α is taken as the type I error probability. The OC curve would represent then the type II error probability, that is, the probability of not detecting a given shift in the prescribed distribution as a function of

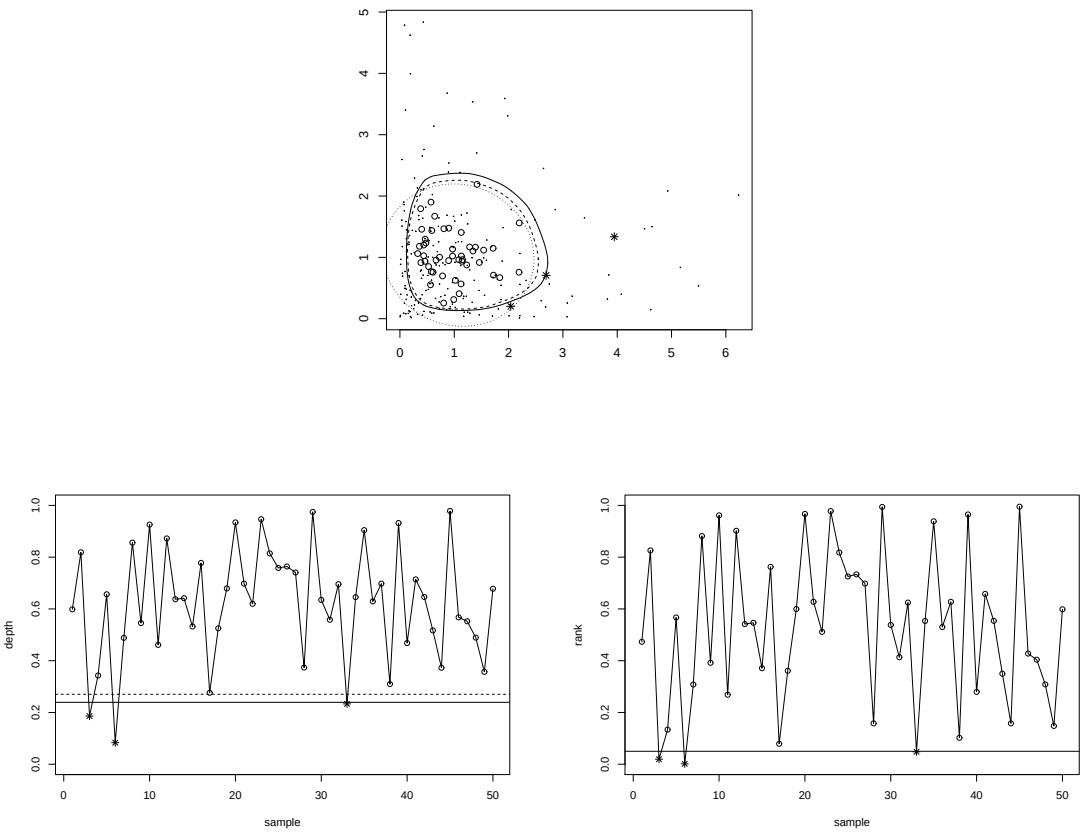

Figure 9: D_μ-chat and r-chart for bivariate Exponential data (bottom) with corresponding region (top).

the magnitude of the shift.

6.1. Shift in location, D_μ*-chart*

If the quality characteristic follows a normal distribution, the D_μ-chart is asymptotically equivalent to the $\overline{X}$-chart. In Figure 10 we compare the D_μ-chart with the Q-chart proposed in [14] to monitor an average rank, see (8). The solid line corresponds to the OC curve of the D_μ-chart with $\alpha = 0.0027$ and sample size $k = 2$ and the dashed line represents the one of the Q-chart with the same α and sample size. The D_μ-chart is more sensible than the Q-chart at detecting shifts in the mean because it aggregates (by averaging) all individual observations from the rational sample, while the Q-chart averages the ranks of the observations.

6.2. Shift in scale, D_σ*-chart*

In Figure 11 we compare the D_σ-chart with the chi-square S-chart under Gaussianity. The solid line corresponds to the OC curve of the D_σ-chart with $\alpha = 0.05$ and sample size $k = 5$, while the dashed line represents the OC curve of the S-chart (which is the one of the usual two-sided test

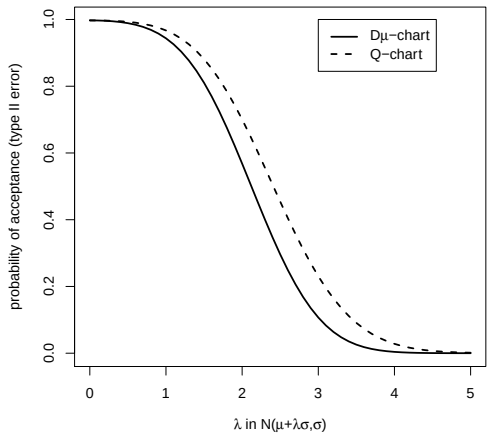

Figure 10: OC curves of D_μ-chart (solid) and Q-chart (dashed) for $k = 2$ and $\alpha = 0.0027$. Axis X represents shifts in location as a number of standard deviations and axis Y the probability that a sample falls in the in-control region. In the in-control state, the quality characteristic follows a normal distribution with parameters (μ_0, σ_0), while after a shift of magnitude λ, its parameters are $(\mu_0 + \lambda\sigma_0, \sigma_0)$.

on the standard deviation). For this specific sample size, the performance of both control charts is very similar. As seen in the chart, when $k = 5$, the D_σ-chart behaves better at detecting increments on the standard deviation (the solid line is below the dashed line to the left of $\lambda = 1$), while the S-chart is better at detecting decrements.

6.3. Shift in location and scale, $D_{(\mu,\sigma)}$*-chart*

In Figure 12 we compare the OC curves of the $D_{(\mu,\sigma)}$-chart for $\delta = 1$ (thin solid line) and $\delta = 0.5$ (thick solid line) in both cases $\alpha = 0.05$, with other alternatives under various shifts on the in-control distribution, which is assumed to be normal. The alternatives are the $\overline{X}$-chart with $\alpha = 0.05$ (thick dashed line), the two-sided (resp. one-sided) chi-square S-chart with $\alpha = 0.05$ (thin dotted line, resp. thick dotted line), and the combination of the $\overline{X}$-chart with $\alpha = 0.025$ and the two-sided (resp. one-sided) chi-square S-chart with $\alpha = 0.025$ (thin dash-dot line, resp. thick dash-dot line).

In the top left chart ($k = 5$) a shift in location measured in a number of standard deviations is considered, in the top right chart ($k = 5$) a shift in scale measured in a multiplication factor, in the bottom left chart ($k = 5$) a simultaneous shift in location and scale to a normal distribution with mean $\mu_0 + 2(\lambda - 1)\sigma_0$ and standard deviation $\lambda\sigma_0$, and the OC curve of the bottom right chart corresponds to a shift in location measured in a number of standard deviations when samples of size $k = 10$ are monitored.

Remark 6.1. Observe that a decay in the standard deviation cannot not be detected in the $D_{(\mu,\sigma)}$ chart for $\delta = 0.5$ as seen in the top right chart of Figure 12. A chart built for greater values of δ, e.g. $\delta = 1/\sqrt{2}$, would be enable its detection.

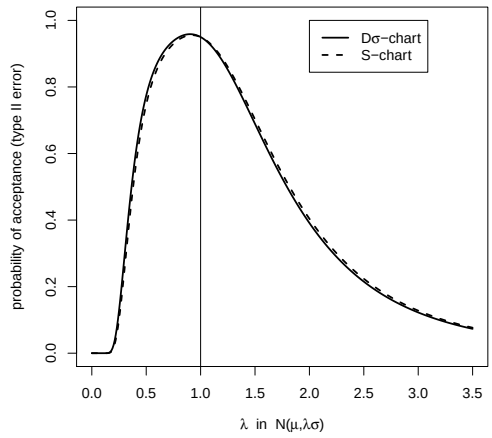

Figure 11: OC curves of D_σ-chart (solid) and chi-square S-chart (dashed) for $k = 5$ and $\alpha = 0.05$. Axis X represents shifts in scale as a multiplication factor and axis Y the probability that a sample falls in the in-control region. In the in-control state, the quality characteristic follows a normal distribution with parameters (μ_0, σ_0), while after a shift of magnitude λ, its parameters are $(\mu_0, \lambda\sigma_0)$.

6.4. $D_{(\mu,\sigma)}$*-chart vs. exact* 2-D *chart*

Chao and Cheng [18] extensively discuss the advantages of using a unique chart to jointly monitorize location and scale. In order to do so, they build the so-called 2-D chart based on the statistic

$$\left(\frac{\overline{X} - \mu_0}{\sigma_0}\right)^2 + \frac{S_k^2}{\sigma_0^2} - \left(1 - \frac{2}{k}\right) \log \frac{\frac{k}{k-1} S_k^2}{\sigma_0^2}\,, \tag{13}$$

whose distribution can be calculated under the assumption of normality. As usual $\overline{X}$ and S_k^2 are the sample mean and sample (not bias-corrected) variance of a sample of size k, while μ_0 and σ_0^2 are the in-control mean and variance which are estimated from the historical dataset. The control region of the 2-D chart is optimal in the sense that for the given significance level, α, has the smallest area in the (X, S) plane for location and scale.

For a given shift in a population distribution, the Average Run Length (ARL) is the the mean number of samples until it is detected in a control chart. It is the inverse of the complementary of the non-detection probability represented in an OC curve, but often preferred to it as an indicator of the performance of a control chart. By means of numerical integration methods, we have compared the ARLs of the 2-D chart with the ones of the $D_{(\mu,\sigma)}$-chart for $\delta = 1$, $\delta = 0.7$, and $\delta = 0.5$ and other classical charts in the presence of small shifts in location, scale, and simultaneous shifts in location and scale.

Table 3 gathers the ARLs until a shift is detected when the in-control distribution is standard normal, the in-control ARL is set at $\mathrm{ARL}_0 = 100$ (which corresponds to $\alpha = 0.01$), and the control is performed on samples of size $k = 5$. The values presented in column 2-D of Table 3 have been

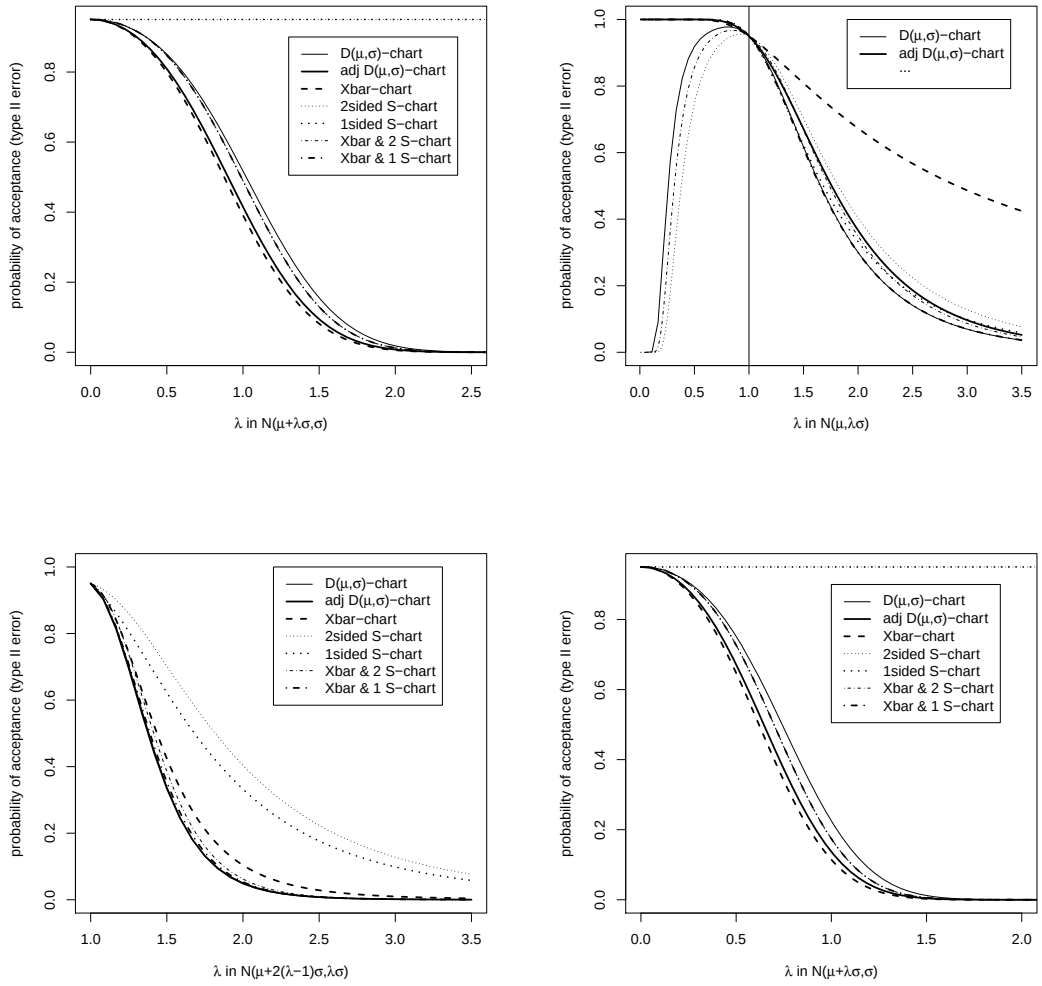

Figure 12: OC curves of $\mathrm{D}_{(\mu,\sigma)}$-charts for $k = 5$ and $\alpha = 0.05$. Axis X represents the shifts either in location, scale or both, measured in several different units, while axis Y represents the probability that a sample falls in the in-control region. In the in-control state, the quality characteristic follows a normal distribution with parameters (μ_0, σ_0), while after a shift of magnitude λ, its parameters are $(\mu_0 + \lambda\sigma_0, \sigma_0)$ (top left), $(\mu_0, \lambda\sigma_0)$ (top right), $(\mu_0 + 2(\lambda - 1)\sigma_0, \lambda\sigma_0)$ (bottom left), and $(\mu_0 + \lambda\sigma_0, \sigma_0)$ for a sample of size $k = 10$ (bottom right).

extracted from Tables 7, 8, and 9 in [18] whenever available there and obtained by the authors by numerical methods otherwise. The 2-D control limit $cl = 2.57$ is the prescribed control limit for the statistic presented in (13) when evaluated on a sample of size $k = 5$ with $\alpha = 0.01$ [see 18, Table 2]. There is a unique column devoted to the $\overline{X}$-chart and D_μ-chart since they are asymptotically equivalent and the ARLs presented in Table 3 are the theoretical ones. Each one of the last two columns is based on the combined usage of two charts, one to track the sample mean and the other to track the sample variance. The significance level of each single chart is set at $\alpha = 0.01/2 = 0.005$,

and the independence of the sample mean and sample variance under Gaussianity guarantees that the probability of rising a false alarm at either of the two charts in absence of assignable causes is approximately 0.01.

μ	σ	$D_{(\mu,\sigma)}$, $\delta = 1$ $d = 0.17724$	$D_{(\mu,\sigma)}$, $\delta = 0.7$ $d = 0.21536$	$D_{(\mu,\sigma)}$, $\delta = 0.5$ $d = 0.22569$	2-D $cl = 2.57$	$\overline{X}$-chart, D_μ $d = 0.30334$	$\overline{X}$-chart and one-sided S	$\overline{X}$-chart and two-sided S
0	1	100.05	99.99	100.01	98.98	100	100.25	100.25
0.1	1	90.36	86.31	84.64	88.22	84.1	90.25	90.25
0.2	1	69.11	60.18	57.37	55.88	55.88	68.2	68.2
0	1.1	39.04	39.62	43.98	40.04	52.09	38.57	47.36
0	1.2	18.31	19.37	23.01	19.03	31.42	18.51	23.55
0.1	1.1	36.52	36.14	39.44	36.68	46.07	36.3	43.98
0.2	1.1	30.4	28.43	29.94	30.66	33.92	30.66	35.92
0.2	1.2	15.52	15.56	17.63	14.9	22.77	16.04	19.65
0.4	1.2	10.47	9.64	10.17	10.58	12.12	11.13	12.7

Table 3: Comparison of ARLs until a shift is detected via exact detection probabilities found by numerical methods, $\text{ARL}_0 = 100$ ($\alpha = 0.01$).

It is remarkable that the behavior of the $D_{(\mu,\sigma)}$-charts considered here are reasonably close to the one of the 2-D chart despite these charts were not built under the consideration of the satisfaction of any optimality property with regard to the normal distribution.

6.5. $D_{(\mu,\sigma)}$*-chart vs.* 2-D, SC, *and* SL*-charts*

Mukherjee and Chakraborti [20] introduce the SL-chart for joint monitorization of the location and scale of the (univariate) ranks of the observations of a sample with respect to a univariate historical dataset, while Chowdhury *et al.* [21] introduce an alternative chart, which they call SC-chart. Since they are based on ranks, these charts are fully nonparametric and distribution-free. We compare them with the $D_{(\mu,\sigma)}$-charts for $\delta = 1$ and $\delta = 0.5$ as well as with the D_μ chart, Shewart $\overline{X}$-chart, and the 2-D chart. The comparison is based on simulations of 50000 historical datasets of 100 observations each of a standard normal distribution and the in-control ARL is set at $\text{ARL}_0 = 500$ (equiv. $\alpha = 0.002$). For each historical dataset, samples of size $k = 5$ were taken until an out-of-control situation was detected. In order to make a fair comparison, the control limits d (for D_θ-charts) and cl (for the 2-D chart) were adjusted by simulation. The asymptotic control limit for the $D_{(\mu,\sigma)}$-chart with $\delta = 0.5$ is $d = 0.149$, while the one for the 2-D chart is $cl = 3.22$, see [18, Appendix].

The values presented in Table 4 represent ARLs until a shift is detected, those corresponding with the SL and SC charts were taken from Table III in Chowdhury *et al.* [21].

Unlike Table 3, which contains a unique column for the D_μ-chart and for the $\overline{X}$-chart, Table 4 has one column for each of these two charts. The reason is that, despite they are asymptotically equivalent on a Gaussian distribution, their behavior when built out of a historical dataset can be different one from the other.

μ	σ	$D_{(\mu,\sigma)}$, $\delta = 1$ $d = 0.099$	$D_{(\mu,\sigma)}$, $\delta = 0.5$ $d = 0.147$	D_{μ} $d = 0.205$	Shewart $\overline{X}$ $z_{\alpha/2} = 3.09023$	2-D $cl = 3.16$	SC	SL
0	1	510.0	504.8	504.2	520.1	509.5	509.4	513.0
0.25	1	325.1	263.9	247.3	235.7	276.4	253.6	257.6
0.5	1	114.7	66.8	59.0	54.7	78.4	68.6	66.5
0	1.25	46.7	49.0	72.4	73.9	40.9	74.5	102.9
0	1.5	9.6	12.8	24.7	25.1	9.0	24.3	37.5
0.25	1.25	36.0	34.5	47.4	47.2	30.7	54.9	70.6
0.5	1.25	20.0	16.1	20.0	19.4	16.7	26.2	30.9

Table 4: Comparison of ARLs until a shift is detected via simulations based on small samples of historical data, specifically $n = 100$, $\alpha = 0.002$ ($\text{ARL}_0 = 500$).

7. Real data applications

We present below two real data applications of the procedures that have been introduced here. In the first place, a Phase I application with a univariate non-normal dataset is considered and subsequently a Phase I and Phase II application over a multivariate normal process. In both cases, the depth-based control charts that we obtain are compared with other alternative procedures proposed at the SPC literature.

7.1. Univariate skewed data

Cowden [32, Ch. 21] presents a dataset containing 150 historical observations (grouped in 30 samples of 5 units each) of the concentration of residue resulting from a chemical process. The p-value of the Shapiro-Wilk normality test over this dataset is below 10^{-15}, so the normality is rejected for any reasonable significance level. Actually, these observations are heavily (right) skewed and hence the classical Shewart $\overline{X}$-chart is not appropriate here. Three alternative $\overline{X}$-control charts for skewed processes are proposed in [32]. Those charts are based not only on the estimation of the location and scale parameter, but also on the estimated shape (skewness and kurtosis) coefficients and some distribution assumption on the process, which is either approximated by means of a Gram-Charlier expansion or assumed to follow a Pearson Type III distribution (Gamma type). More recently, Chang and Bai [10] proposed a heuristic procedure to build an $\overline{X}$-chart for skewed distributions by applying one weight to the standard deviation when computing the Upper Control Limit and another weight when computing the Lower Control Limit. The UCLs of all these control charts lie between 51.15 and 58.71, while the corresponding LCLs lie between 1.16 and 3.5, while the ones of the classical Shewart (symmetric) $\overline{X}$-chart are established at 41.74 and -4.84 (which can be corrected to 0). This means that for the charts that are sensitive to skewness, all trial sample means do lie in between the control limits, meanwhile for the symmetric control chart, samples #8 and #22 are out-of-control, see Figure 13 left for the sample means of all 30 samples.

We have followed the procedure explained in Section 3 in order to estimate the control limit of the D_{μ} chart with $\alpha = 0.0027$ (100000 bootstrap samples of size 5) and have obtained a control

limit $d_\alpha = 0.1475$. In Figure 13 right, we have presented the corresponding D_μ-chart with the control limit represented with a solid line and the control limit in case the normality would not have been rejected (namely 0.22163, see Table 5) as a dotted line. In Figure 13 left, the evolution of the sample means is plotted together with the control limits obtained as the extreme values of the corresponding μ-depth regions and the historical average as a dashed line. It is remarkable that the control limits that are obtained here (solid lines) are 58 and 3 which lie between the ranges of the control limits of the previously described skewed charts. Furthermore, they are almost coincident with the Pearson Type III control limits which were estimated under strong distributional assumptions, meanwhile our control limits are completely data-driven and were built without making any distribution assumption. The dotted lines represent the depth-based control limits under normality. It is also remarkable that these normal control limits, despite they are quite far from the previous ones, do also capture the lack of symmetry of our historical dataset.

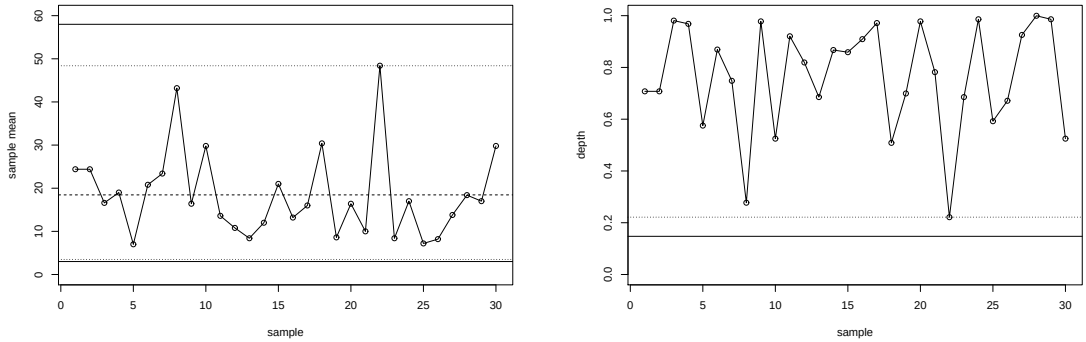

Figure 13: $\overline{X}$-chart based on the μ-depth (left) and D_μ-chart (right).

Commonly Phase I applications are completed with a variability chart. For this reason, we build a D_σ-chart for the chemical process dataset. Due to the lack of normality of the dataset, we apply again Section 3 for the D_σ-chart with $\alpha = 0.0027$ (100000 bootstrap samples of size 5) and obtain $d_\alpha = 0.0675$. In Figure 14 right, we have represented the evolution of the σ-depths of the (not-bias corrected) sample standard deviations with the control limit represented as a solid line. The dotted line there corresponds to the control limit under assumption of normality (see Table 6). On the left, the evolution of the sample standard deviations is monitored. This chart, after a change in scale, is almost coincident with Tsai and Wu [11, Fig. 4] who propose a control chart to monitor the range of a skewed distribution based on weighted standard deviations.

In order to show all the introduced charts in action, we also present the $D_{(\mu,\sigma)}$-chart for S_k. In this case we take $\alpha = 0.0054$ and after 100000 bootstrap samples, the obtained control limit is $d = 0.06578$. In Figure 15 right, we have represented the evolution of the (μ, σ)-depths of $(\overline{X}, S_k)$ with the control limit represented as a solid line. The dashed line corresponds to the median depth which was also approximated by means o a bootstrap procedure, at level $d = 0.651342$. On the

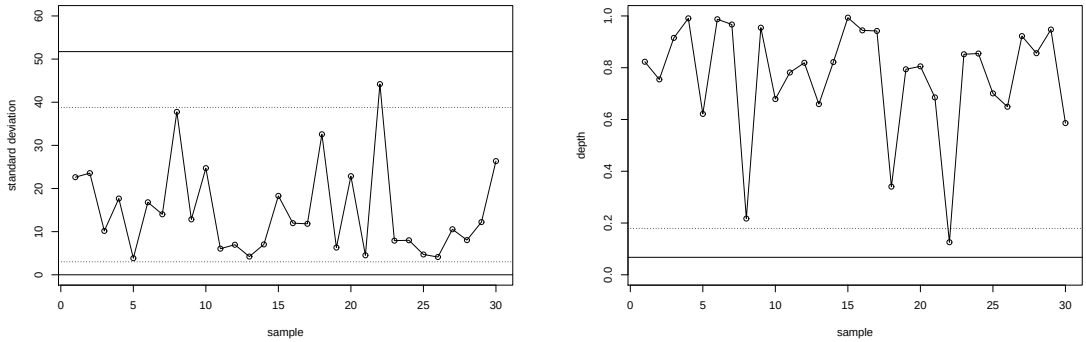

Figure 14: S-chart based on the σ-depth of S_k (left) and D_σ-chart (right).

left, the (μ, σ)-trimmed region of level $d = 0.06578$ is represented with a solid contour. The dashed line is the contour of the region that corresponds to the median depth.

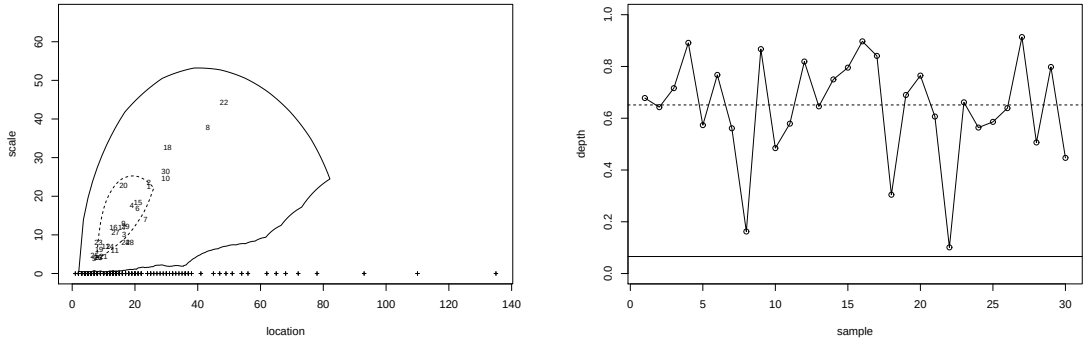

Figure 15: $(\overline{X}, S_k)$-chart based on the (μ, σ)-depth (left) and $\mathrm{D}_{(\mu,\sigma)}$-chart (right).

In conclusion, at the light of the D_μ and D_σ charts used in combination, or the $\mathrm{D}_{(\mu,\sigma)}$ chart used on its own, the chemical process was stable while the trial samples were taken.

7.2. Multivariate observations

The R package `MSQC`, see Santos-Fernandez [33], contains two datasets with three quality characteristics (inner diameter, thickness, and length) $= (X_1, X_2, X_3)$ of carbon fiber tubes. The first dataset is the historical one and contains 30 trial samples of size 8 for Phase I, while the second contains 25 more samples also of size 8 for Phase II. The historical dataset follows a multivariate normal distribution (both Mardia tests on multivariate normality, the one for the skewness and the one for the kurtosis, result in p-values greater than 0.3), and thus the control limit for the D_μ-chart

is taken from Table 5 ($p = 3$, $k = 8$, and $\alpha = 0.0027$) resulting to be $d_\alpha = 0.22606$. In Figure 16 left we have represented the evolution of the μ-depths of the sample means of the 30 trial samples (to the left of the vertical dotted line). All these depths are above the control limit (at d_α) represented by the horizontal solid line. This means that the process has remained stable while they were taken, and there is no need to delete any of them during the building of the control limit following the steps described in Section 3. We checked the stability of this control limit by estimating, as it is prescribed for data from an unknown distribution, and the obtained value (100000 bootstrap samples of size 8) was 0.2233, which is very close to d_α and leads to the same final conclusions. The dashed horizontal line corresponds to the depth of the region whose probability content is 0.5, so half of the depths obtained in the in-control sate are above it, and half below it. To the right of the dotted vertical line (Phase II), we represented the depths of the sample means of the posterior 25 samples with regard to the historical dataset. Sample #34, which is the fourth in this second group, is marked as out-of-control. In Figure 16 right, we represented the Hotelling T^2-chart for this same application, also with Phase I and Phase II and the conclusions obtained from it are the same. Observe that the chart on the left is very similar to the one on the right after upside down reflection

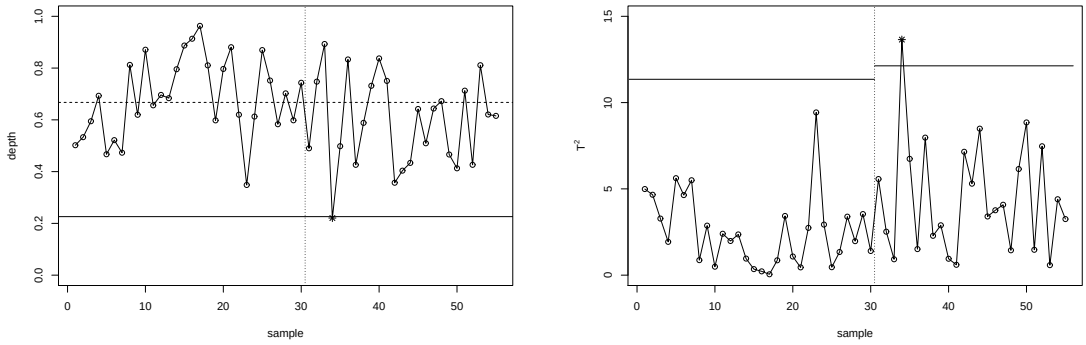

Figure 16: D_μ-chart (left) and Hotelling T^2 chart (right).

In multivariate quality control, once an alarm is risen, it is very important to determine which variable caused such alarm. The multivariate μ-depth of a point is the infimum of the univariate μ-depths over all possible projections, see (7). The μ-depth of the sample mean of sample #34 matches the μ-depth of $0.67113X_1 - 0.71676X_2 - 0.1893X_3$. If this specific projection would have been for monitoritation with the univariate D_μ-chart, the control limit would have been set at 0.34877 (see Table 5 for $p = 1$, $k = 8$, and $\alpha = 0.0027$) and only this sample would have been detected as out-of-control. The depth of sample #23 is 0.3483784 which is slightly below that control limit, but such depth does not correspond to the previous projection.

8. Final remak, conclusions, and extensions

We have introduced multivariate control charts based on the μ-depth and univariate control charts to monitor scale and location-scale parameters based on some transformations of the μ-depth. As a general consideration on multivariate control charts, Jackson [34, Sec. 1.7.3] points out that "Any multivariate quality control procedure ... should fulfill four conditions: 1. A single answer should be available to answer the question: Is the process in control? 2. An overall Type I error should be specified. 3. The procedure should take into account the relationships among the variables. 4. Procedures should be available to answer the question: If the process is out-of-control, what is the problem?", where condition 4. is the most complicated one. It is clear that conditions 1. to 3. are fulfilled in a completely satisfactory way in all charts presented here, whereas condition 4. can be interpreted either as the identification of the variable or set of variables who are responsible for the out-of-control situation or alternatively as the identification of a particular linear combination of variables that is out-of-control. It could well be the case that all individual variables are in-control, but there is an out-of-control situation due to their joint behaviour. As seen in equation (7), the multivariate μ-depth is the infimum (minimum) of all univariate μ-depths over all linear combinations. For that given linear combination of variables, the univariate μ-chart would also detect an out-of-control situation.

In the current manuscript we have introduced the D_θ-charts for the monitorization of the estimates of a parameter θ on subsequent samples of the production based on their parameter depths D_θ with respect to some historical dataset. Special emphasis has been placed on the charts for the mean (μ), standard deviation (σ), and bivariate parameter (μ, σ). The exact control limits of these charts have been computed under the assumption of Gaussianity of the historical (in-control) dataset, while a general distribution-free procedure based on parameter ranks is also described together with the theoretical results that support its validity. The performance of the new control charts has been compared with the one of other existing control charts (both parametric and non-parametric) by means of Operating Characteristic Curves and Average Run Length tables when the (Gaussian) in-control distribution is known, and also when only a small historical dataset is available. The performance is, in both cases, good, despite the procedure presented here is not specific for the normal distribution, but can be applied to any other distribution model. This fact leads us to suggest their usage in the very frequent situation at which the Gaussianity of the in-control data cannot be guaranteed.

The current proposal can be extended to other parameters θ, such as the covariance of a bivariate random vector either on its own, or together with more parameters. Even the whole covariance matrix of a random vector can be taken as the chosen parameter, and a D_Σ-chart can be built. Such a chart would monitorize the covariance matrix in an alternative way to the charts reviewed in Yeh *et al.* [35]. It is also possible to consider the parameter given by the mean vector and covariance matrix in order to build a $D_{(\mu,\Sigma)}$-chart, like the ones described in Reynolds and Cho [36]. Alternatively, it is also possible to consider a functional θ composed by two (or more) location parameters as (θ_1, θ_2), such a functional would not only contain information about the location,

but also about more features of the distribution. Another alternative, somewhat related to Ciupke [17], is to consider set-valued parameters θ, like a data depth-trimmed region at some given level.

Acknowledgements

The authors gratefully acknowledge the support of the Spanish Ministry of Science and Innovation under grants ECO2015-66593 and MTM2015-63971-P and the Principado de Asturias under grant FC-15-GRUPIN14-101.

[1] I. Cascos, Data depth: multivariate statistics and geometry, in: W.S. Kendall, I. Molchanov (Eds.), New Perspectives in Stochastic Geometry, Oxford University Press, 2010, pp. 398–423.

[2] R. Liu, On a notion of data depth based on random simplices, Ann. Stat. 18 (1990) 405–414.

[3] R. Liu, J. Parelius, K. Singh, Multivariate analysis by data depth: Descriptive statistics, graphics and inference (with discussion and a rejoinder by Liu and Singh), Ann. Stat. 27 (1999) 783–858.

[4] J.W. Tukey, Mathematics and the picturing of data, in: R.D. James (Ed.), Proceedings of the 1974 International Congress of Mathematitians (Vol. 2), 1975, pp. 523–531.

[5] Y. Zuo, R. Serfling, General notions of statistical depth function, Ann. Stat. 28 (2000) 461–482.

[6] I. Cascos, M. López-Díaz, Trimmed regions induced by parameters of a probability, J. Multivar. Anal. 107 (2012) 306–318.

[7] I. Mizera, C.H. Müller, Location-scale depth (with discussion), J. American Stat. Associat. 99 (2004) 949–989.

[8] D.C. Montgomery, Introduction to Statistical Quality Control, sixth ed., John Wiley & Sons, New York, 2009.

[9] T-R. Tsai, Skew normal distribution and the design of control charts for averages, Int. J. Reliab. Qual. Saf. Eng. 14 (2007) 49–63.

[10] Y.S. Chang, D.S. Bai, Control charts for positively-skewed populations with weighted standard deviations, Qual. Reliab. Eng. Int. 17 (2001) 397–406.

[11] T-R. Tsai, S-J. Wu, Adjusted weighted standard deviation R chart for skewed distributions, Braz. J. Probab. Stat. 22 (2008) 9–22.

[12] J. Frost, K. Keller, J. Lowe, T. Skeete, S. Walton, J. Castille, N. Pal, A note on interval estimation of the standard deviation of a gamma population with applications to statistical quality control, Appl. Math. Model. 37 (2013) 2580–2587.

[13] Y.S. Chang, D.S. Bai, Multivariate T^2 Control Chart for Skewed Populations Using Weighted Standard Deviations, Qual. Reliab. Eng. Int. 20 (2004) 31–46.

[14] R. Liu, Control Charts for Multivariate Processes, J. American Stat. Associat. 90 (1995) 1380–1387.

[15] R. Liu, K. Singh, Notions of Limiting P Values Based on Data Depth and Bootstrap, J. American Stat. Associat. 92 (1997) 266–277.

[16] R.C. Bell, L.A. Jones-Farmer, N. Billor, A Distribution-Free Multivariate Phase I Location Control Chart for Subgrouped Data from Elliptical Distributions, Technometrics 56 (2014) 528–538.

[17] K. Ciupke, Multivariate Process Capability Index Based on Data Depth Concept, Qual. Reliab. Eng. Int. 32 (2016) 2443–2453.

[18] M-T. Chao, S.W. Cheng, On 2-D Control Charts, Qual. Technol. Quant. Manag. 5 (2008) 243–261.

[19] A.K. McCracken, S. Chakraborti, Control charts for joint monitoring of mean and variance: an overview, Qual. Technol. Quant. Manag. 10 (2013) 17–36.

[20] A. Mukherjee, S. Chakraborti, A distribution-free control chart for the joint monitoring of location and scale, Qual. Reliab. Eng. Int. 28 (2012) 335–352.

[21] S. Chowdhury, A. Mukherjee, S. Chakraborti, A new distribution-free control chart for joint monitoring of unknown location and scale parameters of continuous distributions, Qual. Reliab. Eng. Int. 30 (2014) 191–204.

[22] S-F. Yang, Using a new VSI EWMA average loss control chart to monitor changes in the difference between the process mean and target and/or the process variability, Appl. Math. Model. 37 (2013) 7973–7982.

[23] G. Koshevoy, K. Mosler, Zonoid trimming for multivariate distributions, Ann. Stat. 25 (1997) 1998–2017.

[24] I. Cascos, M. López-Díaz, Consistency of the α-trimming of a probability. Applications to central regions, Bernoulli 14 (2008) 580–592.

[25] O. Pokotylo, P. Mozharovskyi, R. Dyckerhoff, Depth and depth-based classification with R-package ddalpha, 2016, `arXiv:1608.04109v1 [stat.CO]`.

[26] K. Mosler, Multivariate dispersion, central regions and depth. The Lift Zonoid Approach, Lecture Notes in Statistics (Vol. 165) Springer, Berlin, 2002.

[27] I. Cascos, M. López-Díaz, On the uniform consistency of the zonoid depth, J. Multivar. Anal. 143 (2016) 394–397.

[28] R. Liu, K. Singh, A Quality Index Based on Data Depth and Multivariate Rank Tests, J. American Stat. Associat. 88 (1993) 252–260.

[29] R. Liu, K. Singh, J.H. Teng, DDMA-charts: Nonparametric multivariate moving average control charts based on data depth, Allg. Stat. Arch. 88 (2004) 235–258.

[30] R. Liu, J. Tang, Control Charts for Dependent and Independent Measurements Based on Bootstrap Methods, J. American Stat. Associat. 91 (1996) 1694–1700.

[31] A. Azzalini, A. Dalla Valle, The multivariate skew-normal distribution, Biometrika 83 (1996) 715–726.

[32] D.J. Cowden, Statistical Method in Quality Control, Prentice-Hall, Englewood Cliffs, NJ, 1957.

[33] E. Santos-Fernandez, MSQC: Multivariate Statistical Quality Control, 2016, `https://cran.r-project.org/web/packages/MSQC/`.

[34] J.E. Jackson, A User's Guide to Principal Components, John Wiley & Sons, New York, 1991.

[35] A. Yeh, D. Lin, R. McGrath, Multivariate Control Charts for Monitoring Covariance Matrix: A Review, Qual. Technol. Quant. Manag. 5 (2006) 415–436.

[36] M.R. Reynolds, G-Y. Cho, Multivariate Control Charts for Monitoring the Mean Vector and Covariance Matrix, J. Qual. Technol. 38 (2006) 230–253.

Appendix

$p = 1$

$k \backslash \alpha$	0.5	0.1	0.05	0.01	0.0027
1	0.57965	0.1255	0.06363	0.01297	0.00353
2	0.71355	0.29806	0.20503	0.08674	0.04339
3	0.77335	0.40915	0.31313	0.17044	0.10494
4	0.80851	0.48472	0.39211	0.24302	0.16639
5	0.83214	0.53965	0.45182	0.30334	0.22163
6	0.84932	0.58162	0.49858	0.3535	0.26995
7	0.86249	0.6149	0.5363	0.39568	0.31201
8	0.87297	0.64205	0.56746	0.43161	0.34877
9	0.88156	0.6647	0.59371	0.46259	0.38109
10	0.88875	0.68394	0.61618	0.4896	0.40971
11	0.89488	0.70052	0.63566	0.51339	0.43522
12	0.90018	0.715	0.65276	0.53451	0.45812
13	0.90481	0.72777	0.6679	0.55341	0.4788
14	0.90891	0.73913	0.68142	0.57045	0.49756
15	0.91257	0.74932	0.69359	0.58589	0.51469

$p = 2$

$k \backslash \alpha$	0.5	0.1	0.05	0.01	0.0027
1	0.29137	0.04084	0.01858	0.00315	0.00077
2	0.47848	0.161	0.10521	0.04084	0.0194
3	0.57615	0.26371	0.19524	0.10059	0.05996
4	0.63719	0.3424	0.27033	0.161	0.10768
5	0.67955	0.40346	0.33138	0.21568	0.15477
6	0.71099	0.45208	0.38147	0.26371	0.19847
7	0.73542	0.49175	0.4232	0.30566	0.23811
8	0.75507	0.5248	0.45849	0.3424	0.27382
9	0.77128	0.55282	0.48876	0.37477	0.30596
10	0.78492	0.57692	0.51503	0.40346	0.33495
11	0.79661	0.59791	0.53809	0.42907	0.36117
12	0.80674	0.61639	0.55851	0.45208	0.385
13	0.81564	0.6328	0.57674	0.47287	0.40674
14	0.82353	0.64749	0.59313	0.49175	0.42665
15	0.83058	0.66074	0.60797	0.50899	0.44496

$p = 3$

$k \backslash \alpha$	0.5	0.1	0.05	0.01	0.0027
1	0.15475	0.01606	0.00675	0.001	0.00022
2	0.33493	0.09729	0.06122	0.02224	0.01014
3	0.44494	0.18477	0.13349	0.0659	0.03826
4	0.51818	0.25889	0.20074	0.11588	0.07604
5	0.57079	0.31969	0.25887	0.16442	0.11624
6	0.61069	0.36985	0.30845	0.20901	0.15539
7	0.64216	0.41179	0.35088	0.24918	0.19213
8	0.66774	0.44737	0.38748	0.28518	0.22606
9	0.68902	0.47795	0.41935	0.31744	0.25717
10	0.70706	0.50454	0.44735	0.34645	0.28565
11	0.72257	0.5279	0.47216	0.37264	0.31175
12	0.7361	0.54862	0.49431	0.39638	0.33569
13	0.74801	0.56713	0.51422	0.418	0.35773
14	0.7586	0.5838	0.53223	0.43777	0.37805
15	0.76809	0.59889	0.5486	0.45593	0.39686

$p = 4$

$k \backslash \alpha$	0.5	0.1	0.05	0.01	0.0027
1	0.08473	0.00689	0.00271	0.00036	0.00007
2	0.23992	0.06186	0.03771	0.01295	0.0057
3	0.35026	0.13446	0.09516	0.04529	0.02569
4	0.42848	0.20188	0.15418	0.08665	0.05591
5	0.48663	0.26009	0.2081	0.12942	0.09029
6	0.53169	0.3097	0.25575	0.17032	0.12527
7	0.56777	0.35212	0.29753	0.20822	0.1591
8	0.59743	0.38871	0.33423	0.24289	0.19103
9	0.6223	0.42056	0.36663	0.27445	0.22081
10	0.64352	0.44854	0.39541	0.30319	0.24846
11	0.66188	0.47333	0.42114	0.3294	0.27405
12	0.67795	0.49545	0.44428	0.35335	0.29776
13	0.69216	0.51533	0.46521	0.37533	0.31973
14	0.70483	0.53331	0.48423	0.39554	0.34014
15	0.71622	0.54967	0.50162	0.4142	0.35913

$p = 5$

$k \backslash \alpha$	0.5	0.1	0.05	0.01	0.0027
1	0.04728	0.00311	0.00115	0.00014	0.00003
2	0.17434	0.04053	0.02403	0.00784	0.00334
3	0.27904	0.10007	0.06955	0.03204	0.0178
4	0.358	0.16034	0.12083	0.06629	0.04212
5	0.41874	0.21495	0.17018	0.10385	0.07159
6	0.46684	0.26295	0.21526	0.14115	0.1028
7	0.50593	0.30489	0.25571	0.17661	0.13383
8	0.53842	0.34163	0.29186	0.20968	0.16373
9	0.56589	0.37399	0.32418	0.24025	0.19208
10	0.58949	0.4027	0.35319	0.26839	0.2187
11	0.61002	0.42832	0.37934	0.2943	0.24362
12	0.62806	0.45134	0.40302	0.31818	0.26688
13	0.64408	0.47214	0.42456	0.34021	0.2886
14	0.6584	0.49104	0.44424	0.36061	0.30889
15	0.67131	0.50829	0.4623	0.37952	0.32787

$p = 6$

$k \backslash \alpha$	0.5	0.1	0.05	0.01	0.0027
1	0.02672	0.00145	0.00051	0.00005	0.00001
2	0.12794	0.02711	0.01567	0.00488	0.00202
3	0.22413	0.07563	0.0517	0.02312	0.0126
4	0.30127	0.12896	0.096	0.05153	0.03228
5	0.36264	0.17957	0.1408	0.08445	0.05757
6	0.41231	0.22539	0.18305	0.11832	0.08539
7	0.45328	0.26625	0.2218	0.15135	0.11381
8	0.48769	0.30259	0.25699	0.18271	0.14173
9	0.51705	0.33498	0.28886	0.2121	0.16858
10	0.54243	0.36397	0.31775	0.23947	0.19412
11	0.56462	0.39004	0.34399	0.26489	0.21824
12	0.58422	0.41361	0.36791	0.28849	0.24094
13	0.60168	0.43501	0.38979	0.31041	0.26228
14	0.61734	0.45455	0.40988	0.3308	0.28233
15	0.63149	0.47245	0.42839	0.3498	0.30118

Table 5: Gaussian control limit of D_μ-chart, dimension p, sample size k, and false alarm probability α.

	S_k						S_{k-1}				
$k \backslash \alpha$	0.5	0.1	0.05	0.01	0.0027	$k \backslash \alpha$	0.5	0.1	0.05	0.01	0.0027
2	0.53956	0.1175	0.05981	0.01218	0.0033	2	0.53481	0.10656	0.05318	0.01061	0.00286
3	0.70552	0.31561	0.22556	0.10397	0.05528	3	0.69116	0.26886	0.18055	0.07288	0.03531
4	0.77223	0.42605	0.33409	0.19342	0.12553	4	0.75726	0.3662	0.26974	0.13568	0.07912
5	0.80943	0.49331	0.40258	0.2556	0.17922	5	0.79527	0.42995	0.33179	0.18684	0.11999
6	0.83369	0.53888	0.44945	0.29958	0.21862	6	0.82055	0.47561	0.37787	0.22866	0.15619
7	0.851	0.57212	0.48382	0.33273	0.24937	7	0.83884	0.5104	0.41394	0.26366	0.1881
8	0.86412	0.59769	0.51039	0.35922	0.27485	8	0.85284	0.53811	0.4433	0.29359	0.21639
9	0.87448	0.61812	0.53178	0.38137	0.29684	9	0.86396	0.5609	0.46789	0.31961	0.24165
10	0.88291	0.63494	0.54956	0.40047	0.31631	10	0.87308	0.58012	0.48894	0.34255	0.26437
11	0.88995	0.64912	0.5647	0.41733	0.33385	11	0.88071	0.59664	0.50728	0.36299	0.28494
12	0.89593	0.66129	0.57786	0.43245	0.34981	12	0.88722	0.61107	0.52348	0.38139	0.30368
13	0.90109	0.6719	0.58949	0.44616	0.36446	13	0.89285	0.62383	0.53795	0.39807	0.32085
14	0.9056	0.68128	0.5999	0.45871	0.37799	14	0.89778	0.63523	0.55098	0.4133	0.33666
15	0.90959	0.68967	0.60932	0.47027	0.39054	15	0.90214	0.64551	0.56283	0.42728	0.35129

Table 6: Gaussian control limit of the D_σ-chart for sample size k and significance level α for S_k left, and for the square root of the bias-corrected sample variance S_{k-1} right.

$k \backslash \alpha$	0.5	0.1	0.05	0.01	0.0054	0.0027
2	0.36164	0.0771	0.04002	0.00843	0.00473	0.00241
3	0.51872	0.21356	0.15097	0.06989	0.05213	0.03731
4	0.59677	0.29978	0.23109	0.13056	0.10524	0.08387
5	0.6457	0.35813	0.28686	0.17724	0.14873	0.12293
6	0.67987	0.40138	0.3294	0.21563	0.18385	0.15508
7	0.70549	0.43478	0.36245	0.24549	0.21275	0.18295
8	0.72566	0.46202	0.39027	0.27179	0.23901	0.20783
9	0.74214	0.4847	0.41323	0.29563	0.26192	0.22962
10	0.75586	0.5041	0.43349	0.31611	0.28177	0.24979

Table 7: Gaussian control limit of the $D_{(\mu,\sigma)}$-chart based on $(\overline{X}, S_k)$ for sample size k and sig. level α (control limits for $k = 5, \ldots, 10$ obtained by numerical integration, control limits for $k = 2, 3, 4$ approximated after 10^6 simulations).

$k \backslash \alpha$	0.5	0.1	0.05	0.01	0.0054	0.0027
2	0.64406	0.23781	0.1596	0.06538	0.0469	0.03226
3	0.68939	0.32266	0.24157	0.12667	0.0992	0.07572
4	0.71953	0.38314	0.30249	0.18057	0.14915	0.12029
5	0.74107	0.42806	0.34988	0.22569	0.19233	0.16161
6	0.75811	0.46415	0.38847	0.26501	0.23045	0.19794
7	0.77195	0.49367	0.4205	0.29856	0.26379	0.23026
8	0.78348	0.51847	0.44768	0.32767	0.29297	0.25871
9	0.79329	0.53968	0.47112	0.35342	0.3188	0.28489
10	0.80177	0.5581	0.49159	0.37619	0.34179	0.30784

Table 8: Gaussian control limit of the $D_{(\mu,\sigma)}$-chart based on $(\overline{X}, \sqrt{\delta S_k^2 + (1-\delta)\sigma_0^2})$ for $\delta = 0.5$, sample size k, and sig. level α (control limits for $k = 5, \ldots, 10$ obtained by numerical integration, control limits for $k = 2, 3, 4$ approximated after 10^6 simulations).